

Learning Minimal Neural Specifications

CHUQIN GENG, McGill University, Canada
ZHAOYUE WANG, McGill University, Canada
HAOLIN YE, McGill University, Canada
SAIFEI LIAO, University of Toronto, Canada
XUJIE SI, University of Toronto, Canada

Formal verification is only as good as the specification of a system, which is also true for neural network verification. Existing specifications follow the paradigm of data as specification, where the local neighborhood around a reference data point is considered correct or robust. While these specifications provide a fair testbed for assessing model robustness, they are too restrictive for verifying unseen test data—a challenging task with significant real-world implications. Recent work shows great promise through a new paradigm, neural representation as specification, which uses neural activation patterns (NAPs) for this purpose. However, it computes the most refined NAPs, which include many redundant neurons. In this paper, we study the following problem: Given a neural network, find a minimal (general) NAP specification that is sufficient for formal verification of the network’s robustness. Finding the minimal NAP specification not only expands verifiable bounds but also provides insights into which neurons contribute to the model’s robustness. To address this problem, we propose several exact and approximate approaches. Our exact approaches leverage the verification tool to find minimal NAP specifications in either a deterministic or statistical manner. Whereas the approximate methods efficiently estimate minimal NAPs using adversarial examples and local gradients, without making calls to the verification tool. This allows us to inspect potential causal links between neurons and the robustness of state-of-the art neural networks, a task for which existing verification frameworks fail to scale. Our experimental results suggest that minimal NAP specifications require much smaller fractions of neurons compared to the most refined NAP specifications computed by previous work, yet they can significantly expand the verifiable boundaries to several orders of magnitude larger.

CCS Concepts: • **Do Not Use This Code** → **Generate the Correct Terms for Your Paper**; *Generate the Correct Terms for Your Paper*; Generate the Correct Terms for Your Paper; Generate the Correct Terms for Your Paper.

Additional Key Words and Phrases: Do, Not, Us, This, Code, Put, the, Correct, Terms, for, Your, Paper

ACM Reference Format:

Chuqin Geng, Zhaoyue Wang, Haolin Ye, Saifei Liao, and Xujie Si. 2018. Learning Minimal Neural Specifications. In *Woodstock ’18: ACM Symposium on Neural Gaze Detection, June 03–05, 2018, Woodstock, NY*. ACM, New York, NY, USA, 31 pages. <https://doi.org/XXXXXX.XXXXXXX>

1 INTRODUCTION

The growing prevalence of deep learning systems in decision-critical applications has elevated safety concerns regarding AI systems, such as their vulnerability to adversarial attacks [Dietterich and Horvitz 2015; Goodfellow et al. 2015]. Therefore, the verification of AI systems has become increasingly important and attracted much attention from the research community. The field of neural network verification largely follows the paradigm of software verification – using formal

Permission to make digital or hard copies of all or part of this work for personal or classroom use is granted without fee provided that copies are not made or distributed for profit or commercial advantage and that copies bear this notice and the full citation on the first page. Copyrights for components of this work owned by others than the author(s) must be honored. Abstracting with credit is permitted. To copy otherwise, or republish, to post on servers or to redistribute to lists, requires prior specific permission and/or a fee. Request permissions from permissions@acm.org.

Conference acronym ’XX, June 03–05, 2018, Woodstock, NY

© 2018 Copyright held by the owner/author(s). Publication rights licensed to ACM.

ACM ISBN 978-1-4503-XXXX-X/18/06

<https://doi.org/XXXXXX.XXXXXXX>

methods to verify desirable properties of systems through rigorous mathematical specifications and proofs [Wing 1990]. Nearly all existing works [Huang et al. 2020, 2017a; Katz et al. 2017, 2019; Wang et al. 2021b] follow a “*data as specification*” paradigm, which uses the consistency of local neighborhoods (often L_∞ balls) of reference data points as the specification.

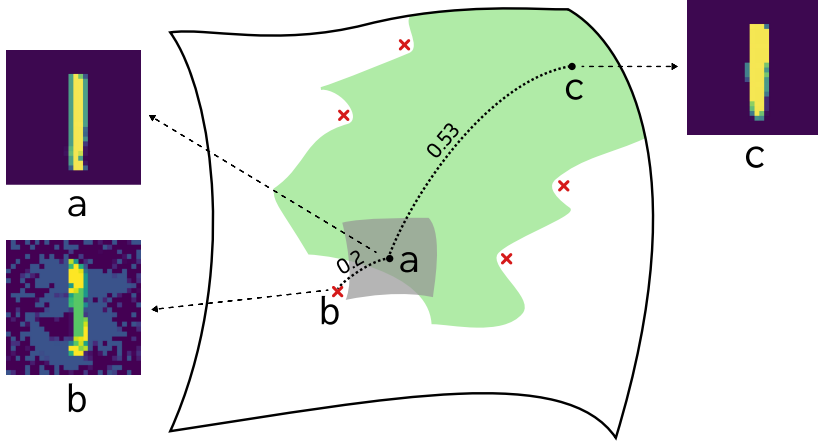


Fig. 1. The comparison between NAP specifications (green region) and L_∞ ball specifications (gray region) on the MNIST dataset. Image a is the reference image, and image c is the closest among all 6000 training images of digit 1, with an L_∞ distance of 0.5294. However, c cannot be verified using the L_∞ ball specification, as an adversarial example b exists at an L_∞ distance of 0.2. Note that this is not a limitation of the underlying verification engines but rather an intrinsic limitation of the specifications. In contrast, NAP specifications allow verification of unseen test set data like c .

While local neighborhood specification provides a fair and effective testbed for evaluating neural networks’ robustness, it has two major limitations: 1) it primarily covers a convex region of input data, which can be mathematically described by adding noise to the reference point, as illustrated in Figure 1b; 2) it is too restrictive to cover unseen test set data, which are real data sampled from the underlying distribution. For instance, the maximum L_∞ verifiable bounds used in VNNCOMP [Brix et al. 2023] – the annual neural network verification competition – are usually less than 0.2, while the smallest distance between data points with the same label exceeds 0.5. Indeed, due to the nature of image distribution, the distances between real images are far beyond L_∞ verifiable bounds. As a result, local neighborhood specifications are not suitable for the verification of unseen test data – a challenging task with significant real-world implications.

To make neural verification practically useful, the desired specification must cover data from the same class, even if they are distributed non-linearly and non-convexly in the input space. Unlike local neighborhood specifications, manually defining such a specification is almost impractical. This poses a tricky chicken-egg problem: machine learning (ML) is necessary because it’s challenging to formally write down a precise definition (aka specification); but to be able to verify machine learning models, a formal specification would be needed. We argue that, in order to tackle this challenge, a separate learning algorithm for specifications is necessary. In this view, the “*data as specification*” paradigm is a simple but extremely overfitted algorithm for specification learning, which simply picks a small neighborhood of a reference data point in the input space. To this end, Geng et al. [2023] proposes using a new and more promising paradigm - “*neural representation as specification*”, which learns a specification in the representation space of the trained machine learning model in the form of neural activation patterns (NAPs). NAPs are abstractions of the values

of hidden neurons which have been shown useful for understanding the decision-making process of a model when making a prediction [Gopinath et al. 2018]. Most importantly, a successful neural network would exhibit similar activation patterns for input data from the same class, regardless of their actual distance in the input space [Bengio et al. 2013; Geng et al. 2023; Tishby and Zaslavsky 2015]. This key observation suggests that if we learn a NAP—a common activation pattern shared by a certain class of data—it can be used as a specification for verifying data from that class. Once such a NAP specification is successfully verified, we say any data covered by this NAP (exhibiting this pattern) provably belongs to the corresponding class. Ideally, if that NAP covers all data from a class, it can be considered a machine-checkable definition of that class. Geometrically speaking, compared to the L_∞ ball specifications, NAP specifications could cover much more flexible and larger regions, as illustrated in Figure 1.

However, it is noteworthy that the current approach to computing NAPs relies on a simple statistical method that assumes each neuron contributes to certifying the robustness of neural networks. Consequently, the computed NAPs are often overly refined. This is a restrictive assumption, as many studies [Frankle and Carbin 2019; Liang et al. 2021; Lu et al. 2019; Wang et al. 2021a] have revealed that a significant portion of neurons in neural networks may not play a substantial role. In the spirit of Occam’s Razor, we aim to systematically remove these redundant neurons that do not affect robustness. This motivates us to address the following challenge: given a neural network, find a minimal (coarsest) NAP that is sufficient for verifying the network’s robustness. This problem is important for the following reasons: i) Minimal NAP specifications cover potentially much larger regions in the input space compared to the most refined ones, increasing the ability to verify more unseen data; ii) Minimal NAP specifications provide insight into which neurons are responsible for the model making robust predictions, helping us to reveal the black-box nature of neural networks. For instance, if we aim to decode NAPs into human-understandable programs or rules [Li et al. 2023], minimal NAPs will always be easier to decipher than the most refined NAPs. We leave interpreting individual neurons as future work.

To find the minimal NAP specifications, we first introduce two basic algorithms: `REFINE` and `COARSEN`. These algorithms exhaustively check all possible candidates using off-the-shelf verification tools, such as Marabou [Katz et al. 2019]. For instance, `COARSEN` gradually coarsens each neuron of the most refined NAPs and retains only the coarsened neurons when Marabou returns a verification success. While these approaches provide correctness guarantees, they are not efficient for verifying large neural networks, as calls to verification tools are typically expensive. To improve efficiency, we further propose statistical variants of `REFINE` and `COARSEN`—`SAMPLE_REFINE` and `SAMPLE_COARSEN` that leverage sampling and statistical learning principles to find the minimal NAP specification.

However, verification-dependent approaches struggle to scale up to state-of-the-art neural network models due to limitations in current verification tools. This motivates us to explore estimation methods that are independent of verification tools. In our exploration, we discover that adversarial examples and local gradients offer valuable insights into mandatory neurons—the essential building blocks of minimal NAPs. Based on these insights, we develop two approximate approaches: `ADVERSARIAL_PRUNE` and `GRADIENT_SEARCH`. Our experimental results demonstrate that these estimation methods produce fairly accurate estimates. Additionally, we apply these methods to state-of-the-art neural networks such as VGG-19 [Simonyan and Zisserman 2014]. Although we cannot formally verify the correctness of these estimated minimal NAP specifications due to the scalability limitations of current verification techniques, we demonstrate that these NAPs capture important hidden features and concepts learned by the model. As many studies indicate, visual interpretability and robustness are inherently related and observed in learned features and representations [Alvarez Melis and Jaakkola 2018; Boopathy et al. 2020; Dong et al. 2017]. Therefore,

we believe that the estimated mandatory neurons can account for the model's robustness and their activation states can also serve as empirical certificaces of a confident prediction.

Moreover, previous research has suggested that NAP specifications cover larger regions than L_∞ ball specifications, but lacks empirical evidence. In this paper, we fill this gap by introducing a simple and efficient method to estimate the volume of certified regions corresponding to NAP specifications. Additionally, this method offers a rough approximation of the volumetric change from refined NAP specifications to minimal NAP specifications. Our contributions can be summarized as follows:

- We propose the problem of learning the minimal NAP specification, emphasizing the necessity for a new paradigm of specifying neural networks. We present two simple verification-based approaches with correctness guarantees, alongside more efficient statistical methods.
- We introduce key concepts including the abstraction function, NAP specification, and mandatory neurons. We show that the problem is equivalent to identifying all mandatory neurons and propose two efficient estimation approaches to learning them.
- Our experiments indicate that the minimal NAP specifications involve significantly fewer neurons compared to the most refined NAPs computed by the baseline approach. Moreover, they expand the verifiable bound by several orders of magnitude.
- We estimate mandatory neurons in the state-of-the-art neural network, VGG-19. By leveraging a modified Grad-CAM map [Selvaraju et al. 2017], we demonstrate that these mandatory neurons are essential for visual interpretability - strong evidence that they may also account for the model's robustness performance.

2 BACKGROUND

In this section, we introduce basic knowledge and notations of adversarial attacks and neural network verification, with an emphasis on verification using NAP specifications. This may help readers better understand the importance of learning minimal NAP specifications.

2.1 Neural Networks for Classification Tasks

In this paper, we focus on feed-forward ReLU neural networks. Generally speaking, a feed-forward network N is comprised of L layers, where each layer performs a linear transformation followed by a ReLU activation. We denote the pre-activation value and post-activation value at the l -th layer as $z^{(l)}(x)$ and $\hat{z}^{(l)}(x)$, respectively. The l -th layer computation is expressed as follows: $z^{(l)}(x) = \mathbf{W}^{(l)}\hat{z}^{(l-1)}(x) + \mathbf{b}^{(l)}$, $\hat{z}^{(l)}(x) = \text{ReLU}(z^{(l)}(x))$, with $\mathbf{W}^{(l)}$ being the weight matrix and $\mathbf{b}^{(l)}$ representing the bias for the l -th layer. We denote the number of neurons in the l -th layer as d_l , and the i -th neuron in layer l as $N_{i,l}$. The pre-activation value and post-activation value of $N_{i,l}$ at input x is computed by $z_i^{(l)}(x)$ and $\hat{z}_i^{(l)}(x)$. The network can also be viewed as a function $F^{<N>} := \mathbb{R}^{d_0} \rightarrow \mathbb{R}^{d_L}$ such that $F^{<N>}(x) := z^{(L)}(x)$, where $F_i^{<N>}(x) := z_i^{(L)}(x)$ represents the output of i -th neuron in the last layer. We will omit N when the context is clear. In multi-class classification with classes C , given input x , the neural network predicts class $c \in C$ if the output $F_c(x)$ of the c -th neuron in the L -th layer is the highest.

2.2 Adversarial Attacks and Neural Networks Verification Problem

Given a neural network F and a reference point x , adversarial attacks aim to search for a point x' that is geometrically close to the reference point x such that x' and x belong to different classes. Here, we use the canonical specification, that is, we want to search in the local neighborhoods (L_∞ norm balls) of x , formally denoted as $B(x, \epsilon) := \{x' \mid \|x - x'\|_\infty \leq \epsilon\}$, where ϵ is the radius. For

certain ϵ , given we know x belongs to class j , we say an adversarial point is found if:

$$\exists x' \in B(x, \epsilon) \quad \exists i \in C \quad F_i(x') - F_j(x) > 0 \quad (1)$$

In practice, the change from the original data x to adversarial data x' should be imperceptible, so they are more likely to be recognized as the same class/label from a human perspective. There are also metrics other than the L_∞ norm to represent the "similarity" between x and x' , such as the L_0 and L_2 norms [Xu et al. 2020]. However, almost all of them fall into the local neighborhood specification paradigm. This is different from the NAP specification, as we will discuss later.

Neural networks are vulnerable to adversarial attacks, where even imperceptible changes can alter predictions significantly. This underscores the critical need for neural network verification, which can be viewed as countering adversarial attacks. Solving the verification problem involves formally proving the absence of adversarial points in $B(x, \epsilon)$. Formally, we seek to verify:

$$\forall x' \in B(x, \epsilon) \quad \forall i \neq j \quad F_j(x') - F_i(x') > 0 \quad (2)$$

For a simpler presentation, we assume that $F(x)$ is a binary classifier. For any given specification, $F(x) \geq 0$ indicates that the model is verified; otherwise, we can find an adversarial example. Solving such a problem is known to be NP-hard [Katz et al. 2017], and achieving scalability in verification remains an ongoing challenge.

2.3 Neuron Abstractions and Neural Activation Patterns

To better discuss NAP specification and robustness verification, we first introduce the relevant concepts of neuron abstractions, neuron abstraction functions, and neural activation patterns.

Neuron Abstractions. Given a neural network N , for an arbitrary internal neuron $N_{i,l}$ where $0 \leq i \leq d_l$ and $1 \leq l \leq L - 1$, its post-activation value $\hat{z}_i^{(l)}(x)$ can be abstracted into finite states. Formally, this can be viewed as a mapping from \mathbb{R} to \mathbb{S} , where \mathbb{S} represents a set of abstraction states $\{s_1, s_2, \dots, s_n\}$. We define the activation using abstraction of values of a neuron output. A straightforward and intuitive abstraction is a binary abstraction on ReLU activation function, consisting of two states s_0 and s_1 , where $s_0 := 0$ and $s_1 := (0, \infty)$. s_0 and s_1 are often referred to as deactivation and activation states. In addition, we can further abstract these two states to a unary state $s_* := [0, \infty)$, where the interval covers the entire range of post-activation. This is essentially an identity mapping of $\hat{z}_i^{(l)}(x)$. It means that the neurons can be in either state s_0 or state s_1 . Formally, we introduce a partial order \leq among the states. $s_0 \leq s_*$ and $s_1 \leq s_*$ indicates that s_* is an abstraction of s_0 and s_1 , and that s_0 and s_1 are refinements of s_* . Clearly, $s_* \leq s_*$. For convenience, we omit s in representation and use 0 , 1 , and $*$ to refer to these abstractions respectively. In principle, our minimal specification learning applies to any activation function provided that activation can be defined within the abstraction domain.

Definition 2.1 (Neuron Abstraction Function). Given a neural network N and the abstraction state set \mathbb{S} . A neuron abstraction function is the mapping $\mathcal{A} : N \rightarrow \mathbb{S}$. Formally, for an arbitrary neuron $N_{i,l}$ where $0 \leq i \leq d_l$ and $1 \leq l \leq L - 1$, the function abstracts $N_{i,l}$ to some state $s_k \in \mathbb{S}$, i.e., $\mathcal{A}(N_{i,l}) = s_k$.

The above characterization of neuron abstraction, it does not instruct us on how to perform binary abstraction in the absence of neuron values. Thus, we include the input(s) x or X as a new parameter in \mathcal{A} , and it is omitted when the context is clear. Here, we discuss three types of \mathcal{A} : the unary abstraction function function \mathcal{A} , the binary abstraction function $\tilde{\mathcal{A}}$, and the statistical abstraction function $\tilde{\mathcal{A}}$.

The unary $\dot{\mathcal{A}}$ function. The unary abstraction function always maps all inputs to the coarsest state $*$. Formally:

$$\dot{\mathcal{A}}(N_{i,l}, x) = * \quad (3)$$

The binary $\ddot{\mathcal{A}}$ function. When an input x is passed through an internal neuron $N_{i,l}$, we can easily determine the binary abstraction state of $N_{i,l}$ based on its post-activation value $\hat{z}_i^{(l)}(x)$. This motivates us to define the binary abstraction function as follows:

$$\ddot{\mathcal{A}}(N_{i,l}, x) = \begin{cases} 0 & \text{if } \hat{z}_i^{(l)}(x) = 0 \\ 1 & \text{if } \hat{z}_i^{(l)}(x) > 0 \end{cases} \quad (4)$$

The statistical $\tilde{\mathcal{A}}$ function. The binary $\ddot{\mathcal{A}}$ function is limited in calculating a single input, and meets a challenge when multiple inputs come into play, as two distinct inputs may lead to disagreements in a neuron's abstraction state. We then approach this problem statistically by introducing the $\tilde{\mathcal{A}}$ function defined as follows:

$$\tilde{\mathcal{A}}(N_{i,l}, X) = \begin{cases} 0 & \text{if } \frac{|\{x_j | \tilde{\mathcal{A}}(N_{i,l}, x_j) = 0, x_j \in X\}|}{|X|} \geq \delta \\ 1 & \text{if } \frac{|\{x_j | \tilde{\mathcal{A}}(N_{i,l}, x_j) = 1, x_j \in X\}|}{|X|} \geq \delta \\ * & \text{otherwise} \end{cases} \quad (5)$$

where δ is a real number from $[0, 1]$, and X represents a set of inputs, i.e., $X := \{x_1, x_2, \dots, x_n\}$. Since datasets often contain noisy data or challenging instances that the model cannot predict accurately, we introduce the parameter δ to accommodate standard classification settings in which Type I and Type II errors are non-negligible. Intuitively, the introduction of δ allows multiple inputs x_1, \dots, x_n to vote on a neuron's state. For instance, when δ is set to 0.99, then 99% or more of the inputs must agree that a neuron is activated for the neuron to be in the 1 state. It is worth mentioning that the statistical $\tilde{\mathcal{A}}$ function is equivalent to the method described in Geng et al. [2023], which will serve as our baseline approach.

Definition 2.2 (Neural Activation Pattern). Given a neural network N and a neuron abstraction function \mathcal{A} . A neural activation pattern (NAP) P is a tuple that consists of the abstraction state of all neurons in N . Formally, $P := \langle \mathcal{A}(N_{i,l}) \mid N_{i,l} \in N, \mathcal{A} \in \{\ddot{\mathcal{A}}, \dot{\mathcal{A}}\} \rangle$, also denoted as $\mathcal{A}(N)$. The neuron $N_{i,l}$'s abstraction state specified by NAP P is represented as $P_{i,l}$, i.e., $P_{i,l} = \mathcal{A}(N_{i,l})$.

Partially ordered NAP. We denote the power set of NAPs in N as \mathcal{P} . The number of all possible NAPs in N scales exponentially as the number of neurons increases. For such a large set, if we aim to find the minimal NAP — the central problem in this work, we first have to establish an order so that NAPs can be compared. To this end, we define the following partial order:

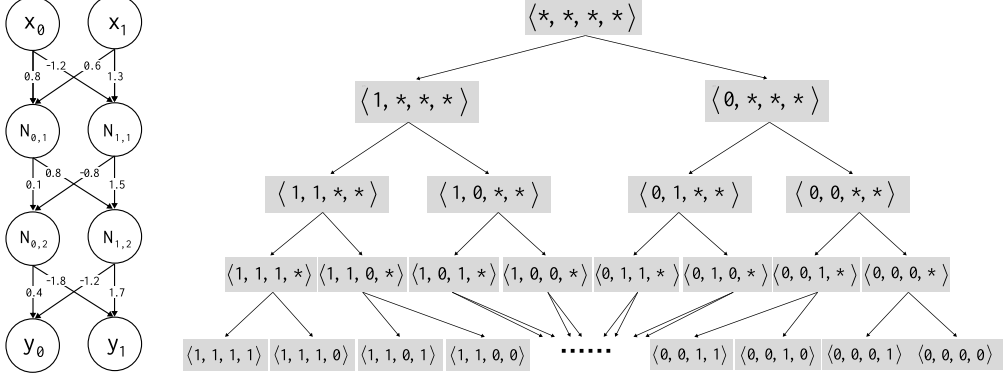
Definition 2.3 (Partially ordered NAP). For any given two NAPs $P, P' \in \mathcal{P}$, we say P' subsumes P if, for each neuron $N_{i,l}$, its state in P is an abstraction of that in P' . Formally, this can be defined as:

$$P' \leq P \iff P'_{i,l} \leq P_{i,l} \quad \forall N_{i,l} \in N \quad (6)$$

Moreover, two NAPs P, P' are equivalent if $P \leq P'$ and $P' \leq P$.

To give a concrete example, Figure 2b depicts a subset of NAPs of a simple neural network consisting of 2 hidden layers and 4 neurons, as presented in Figure 2a.

It is interesting to see that a subset of the NAP \mathcal{P} family can form a complete binary tree given an order of abstraction in neurons. In this example, we use the order of $N_{0,1}, N_{1,1}, N_{0,2}, N_{1,2}$. Setting a different order will create a different tree of NAPs. The root of the tree is the coarsest NAP $\langle *, *, *, * \rangle$. Increasing the depth means that $\tilde{\mathcal{A}}$ applies to more neurons, and when reaching



(a) A simple 2×2 fully connected neural network and a subset of its NAP in a binary tree structure. (b) A subset of the NAP \mathcal{P} family forms a binary tree. Each child subsumes its parent, and fully connected the root is the most abstracted NAP. The leaf node represents the most refined NAPs, where each neuron is either 1 or 0. From the root, the tree is spanned by abstracting each neuron in an order of $N_{0,1}, N_{1,1}, N_{0,2}, N_{1,2}$. Setting a different order will create a different tree of NAPs.

Fig. 2. A simple 2×2 fully connected neural network and a subset of its NAP in a binary tree structure.

the leaf node, all neurons have been abstracted by \mathcal{A} . The leaf nodes represent the most refined NAPs, and there are $2^{|N|}$ of them in total. In addition, each child node always subsumes its parent. By transitivity, a leaf node always subsumes its ancestors along the path. For instance, $\langle 1, 0, 1, 0 \rangle \preccurlyeq \langle 1, 0, 1, * \rangle \preccurlyeq \langle 1, 0, *, * \rangle \preccurlyeq \langle *, *, *, * \rangle$. However, the children under the same parent are not comparable. For instance, $\langle 1, 0, *, * \rangle \preccurlyeq \langle 1, 1, *, * \rangle$. This is because these NAPs sit on different branches formed by splitting certain ReLUs.

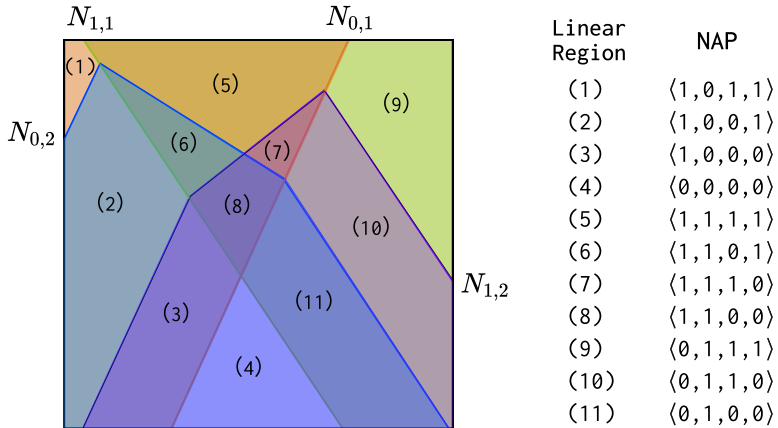


Fig. 3. Linear regions are shattered by the simple 2×2 neural network. Each linear region corresponds to a most refined NAP, but not necessarily vice versa. More abstracted NAPs are formed by ignoring lines/hyperplanes created by neurons.

Region Outlined by NAPs. One key requirement for verification specification is its ability to represent a specific region within the input space. For the canonical local neighbor specifications, these specifications define L_∞ norm balls using explicit formulas like $B(x, \epsilon) := \{x' \mid \|x - x'\|_\infty \leq \epsilon\}$. On the other hand, NAP specifications outline certain regions in the input space implicitly. We define the region specified by P as R_P which is a set of inputs whose activation pattern subsumes the given NAP P . Formally, we have $R_P := \{x \mid \mathcal{A}(N, x) \leq P\}$. To provide a concrete example, Figure 3 illustrates the NAP family of the simple neural network in Figure 2a. These NAPs essentially correspond to regions bounded by hyperplanes created by neurons. The most refined NAPs correspond to individual linear regions from (1) to (11). For example, linear region (9) represents $\langle 0, 1, 1, 1 \rangle$. Since the coarsest state $*$ abstracts the binary states 0 and 1, a NAP with more $*$ covers a larger region in the input space, and this region can be concave. Take the NAP $\langle *, *, 1, * \rangle$ as an example; it corresponds to the union of linear regions (1), (5), (7), (9), and (10). It is interesting to note that the number of linear regions is less than the size of the NAP family. Similar findings have been reported in [Geng et al. 2022; Hanin and Rolnick 2019a,b].

2.4 NAP Specifications for Robustness Verification

This subsection illustrates how NAP specifications can be utilized for robustness verification. We discuss how the abstraction states of neurons can serve as signatures of distinct classes with the introduction of the class NAP definition.

Definition 2.4 (Class NAP). In a classification task with the class set C , for any class $c \in C$, a class NAP P^c is a NAP comprising abstract states outputted by an abstraction function given X_c , where X_c denotes the set of inputs belonging to class c . Formally, $P^c := \langle \mathcal{A}(N_{i,l}, X_c) \mid N_{i,l} \in N, \mathcal{A} \in \{\tilde{\mathcal{A}}, \mathcal{A}\} \rangle$. The power set of P^c is denoted as \mathcal{P}^c .

Recall that robustness verification can be thought of as proving that no adversarial examples exist in the local neighbourhoods of some reference point x . Intuitively, for NAP specifications, it is equivalent to show that no adversarial examples exist in the class NAP P^c ; in other words, inputs exhibiting the NAP P^c must be predicted as class c . Geng et al. [2023] argues that class NAPs must satisfy several essential requirements to qualify as NAP specifications. And finding qualified NAP specifications implies the underlying robustness problem is verified. We formally frame these requirements into the following properties:

The non-ambiguity property. Since we want class NAPs to serve as certificates for a certain class, they must be distinct from each other. Otherwise, there could exist an input that exhibits two class NAPs, which leads to conflicting predictions. Formally, we aim to verify the following:

$$\forall x \quad \forall c_1, c_2 \in C \text{ s.t. } c_1 \neq c_2 \quad \mathcal{A}(N, x) \leq P^{c_1} \implies \mathcal{A}(N, x) \leq P^{c_2} \quad (7)$$

From a geological perspective, there must be no overlaps between class NAPs. In other words, it is also equivalent to verifying:

$$\forall c_1, c_2 \in C \text{ s.t. } c_1 \neq c_2 \quad R_{P^{c_1}} \bigcap R_{P^{c_2}} = \emptyset$$

We empirically observe that successful models, particularly neural networks that have achieved high accuracy in classification tasks, naturally exhibit this property. Because successful models tend to avoid confusion in predictions, their class NAPs are usually very distinct from each other.

The NAP robustness property. To serve as NAP specifications, class NAPs P^c ensure that if an input exhibits it, i.e., $\mathcal{A}(N, x) \leq P, \mathcal{A} \in \{\tilde{\mathcal{A}}, \mathcal{A}\}$, the input must be predicted as the corresponding class c . Formally, we have:

$$\forall x \in R_{P^c} \quad \forall k \in C \text{ s.t. } k \neq c \quad F_c(x) - F_k(x) > 0 \quad (8)$$

in which

$$R_{P^c} = \{x \mid \mathcal{A}(N, x) \leq P^c\} \quad (9)$$

In contrast to canonical L_∞ norm balls, class NAPs are more flexible in terms of size and shape. Additionally, there is no need to specify a reference point, since the locations of potential reference points are also encoded by class NAPs. However, it is possible that no class NAP P^c in \mathcal{P}^c satisfies this property. This can be mitigated by meeting the subsequent weaker property.

The NAP-augmented robustness property. Instead of relying solely on class NAPs as specifications, local neighbours can still be employed in conjunction for verification. This hybrid form of specification has several advantages: 1) It narrows down the scope of verifiable regions when no class NAPs can meet the NAP robustness property; 2) NAP constraints essentially fix ReLU states, refining the search space for verification tools; 3) It focuses on the verification of valid test inputs rather than adversarial examples. Formally, this property can be stated as:

$$\forall x' \in B(x, \epsilon) \bigcap R_{P^c} \quad \forall k \in C \text{ s.t. } k \neq c \quad \mathbf{F}_c(x) - \mathbf{F}_k(x) > 0 \quad (10)$$

in which

$$B(x, \epsilon) = \{x' \mid \|x - x'\|_\infty \leq \epsilon\} \quad R_{P^c} = \{x' \mid \mathcal{A}(N, x') \leq P^c\} \quad (11)$$

To summarize, we state that a class NAP can serve as a NAP specification if it satisfies either the NAP robustness property or the NAP-augmented robustness property. Clearly, the former property is stronger, and it is possible that we can't find a class NAP P^c in \mathcal{P}^c to satisfy this property. Fortunately, we can always find NAPs that satisfy the latter property by narrowing the verifiable region using additional L_∞ norm ball specifications.

3 THE MINIMAL NAP SPECIFICATION PROBLEM

In this section, we formulate the problem of learning minimal NAP specifications and present two naive approaches for solving this problem. Since our approaches require interactions with verification tools, we begin by introducing relevant notations describing the relationships between NAPs and verification tools.

3.1 Problem Formulation

Let (\mathcal{P}^c, \leq) be a partially ordered set corresponding to a family of class NAPs regarding some class $c \in C$. For simplicity, we omit the superscript c and refer to class NAPs simply as NAPs when the context is clear. We assume we have access to a verification tool, $\mathcal{V} : \mathcal{P} \rightarrow \{0, 1\}$, which maps a class NAP $P \in \mathcal{P}$ to a binary set. Here, $\mathcal{V}(P) = 1$ denotes a successful verification of the underlying robustness query, while 0 indicates the presence of an adversarial example. From an alternative perspective, $\mathcal{V}(P) = 1$ also signifies that P is a NAP specification, i.e., it satisfies NAP(-augmented) robustness properties; whereas $\mathcal{V}(P) = 0$ implies the opposite.

It is not hard to see that \mathcal{V} is monotone with respect to the NAP family (\mathcal{P}, \leq) . Given $P \leq P'$ and $\mathcal{V}(P') = 1$, it follows that $\mathcal{V}(P) = 1$. However, given $P \leq P'$ and $\mathcal{V}(P) = 1$, we cannot determine $\mathcal{V}(P')$. In other words, refining a NAP (by increasing the number of neurons abstracted to 0 or 1) can only enhance the likelihood of successful verification of the underlying robustness query.

Definition 3.1 (The minimal NAP specification problem). Given a family of NAPs \mathcal{P} and a verification tool \mathcal{V} , the minimal NAP specification problem is to find a NAP P such that

$$\arg \min_{P \in \mathcal{P}, \mathcal{V}(P)=1} |P|$$

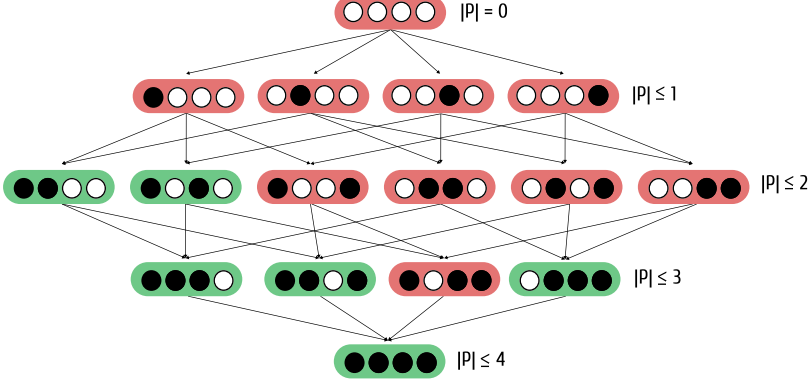


Fig. 4. A DAG representing all possible NAPs, with green nodes signifying they can serve as a specification, while red nodes indicate they cannot. Within each node, a black circle means the corresponding neuron is abstracted by $\tilde{\mathcal{A}}$, whereas the white circle means it is abstracted by $\dot{\mathcal{A}}$. Thus, the top node represents the coarsest NAP, while the bottom node entails the most refined one. Our goal is to find the NAP that resides in the green nodes while its size is minimal.

where $|P|$ is defined as the size of P , representing the number of neurons that are abstracted to the 0 or 1, i.e., $|\{N_{i,l} \mid P_{i,l} = 0 \text{ or } 1\}|$. The (largest) minimal NAP specification's size is denoted as s .

When P is minimal, it implies that for any NAP P' that is strictly more coarse than P , $\mathcal{V}(P') = 0$. Formally, this can be expressed as: $\forall P \preccurlyeq P', P' \neq P : \mathcal{V}(P') = 0$. Thus, there could exist multiple minimal NAP specifications. In such cases, we only need to choose one of them. On the other hand, it is possible that even the most refined NAPs cannot verify the robustness query. In such cases, we claim that no minimal NAP specifications exist. Additionally, since the computation using verification tools is usually expensive, we are interested in methods that efficiently find a minimal NAP specification, i.e., minimizing the number of calls to \mathcal{V} .

We present two naive approaches to solving the problem. Since these approaches involve refining and coarsening the NAP, we will first formally define these two actions.

Refine and Coarsen Action of NAP. Recall our definition of NAP, the coarsest NAP is the one using $\tilde{\mathcal{A}}$ to abstract each neuron in N . We denote this NAP as $\dot{P} := \langle \tilde{\mathcal{A}}(N_{i,l}) \mid N_{i,l} \in N \rangle$. \dot{P} is the smallest NAP with $|\dot{P}| = 0$. In addition, we define the most refined NAP as the one that applies $\tilde{\mathcal{A}}$ to abstract each neuron in N . We denote it as $\tilde{P} := \langle \tilde{\mathcal{A}}(N_{i,l}) \mid N_{i,l} \in N \rangle$. \tilde{P} is the largest NAP with size with $|\tilde{P}| \leq |N|$. Clearly, $\tilde{P} \preccurlyeq \dot{P}$. Given any NAP P , if we want to refine P through a specific neuron $N_{i,l}$, we apply the $\tilde{\mathcal{A}}$ function to $N_{i,l}$. We denote this refinement action as $\tilde{\Delta}(N_{i,l})$. This action will either increase or leave unchanged $|P|$. Similarly, we denote the coarsen action as $\dot{\Delta}(N_{i,l})$. This action will either decrease or leave unchanged $|P|$. We present the semantics of these actions as follows:

$$\begin{array}{c}
 \frac{P \vdash \Delta_1 \Downarrow P' \quad P' \vdash \Delta_2 \Downarrow P''}{P \vdash \cdot \Downarrow P} \quad \text{Refine} \frac{P_{i,l} = *}{P \vdash \tilde{\Delta}(N_{i,l}) \Downarrow \tilde{\mathcal{A}}(N_{i,l}) \cup P \setminus P_{i,l}} \quad \text{Coarsen} \frac{P_{i,l} \in \{0, 1\}}{P \vdash \dot{\Delta}(N_{i,l}) \Downarrow \dot{\mathcal{A}}(N_{i,l}) \cup P \setminus P_{i,l}}
 \end{array}$$

where P, P', P'' are from the NAP family \mathcal{P} , and N is the underlying neural network. Δ_1 and Δ_2 are any two sequences of refine and coarsen actions.

3.2 The Refine Approach

Conceptually, the REFINE approach iteratively increases the number of refined neurons in NAP P until $\mathcal{V}(P) = 1$, i.e., P is able to prove the underlying robustness query. In other words, we gradually increase the size parameter k and iterate over each NAP P of size k to check if $\mathcal{V}(P) = 1$, as illustrated in Algorithm 1. To determine if a solution to the problem exists, we first check if the most refined NAP can succeed in verification. We proceed to iterative refinement only if $\mathcal{V}(\tilde{P}) = 1$. However, the algorithm is not efficient and requires $2^{|N|} - 1$ calls to \mathcal{V} in the worst case, as proven in Theorem 3.2. Please refer to the proof in Appendix A. Therefore REFINE is only practical when the search space of the NAP family \mathcal{P} is small.

Theorem 3.2. *The algorithm REFINE returns a minimal NAP specification with $O(2^{|N|})$ calls to \mathcal{V} .*

Algorithm 1: REFINE

Input: The neural network N
Output: A minimal NAP specification P

```

1 Function Refine( $N$ )
2    $P \leftarrow \tilde{\mathcal{A}}(N)$ 
3   if  $\mathcal{V}(P) == 0$  then
4     return None; /* Return None if even the most refined NAP fails verification */
5   else
6     for  $k$  from 1 to  $|N|$  do
7        $P \leftarrow \tilde{\mathcal{A}}(N)$  /* Refinement starts from the coarsest NAP  $\tilde{P}$  */
8        $K_{\text{comb}} \leftarrow \text{Pick\_K\_Neurons}(k, N)$  /* Returns all combinations of size  $k$  */
9       for  $\text{comb}$  in  $K_{\text{comb}}$  do
10         for  $N_{i,l}$  in  $\text{comb}$  do
11            $P \leftarrow \tilde{\Delta}(N_{i,l})$  /* Refine neurons in the chosen combination */
12           if  $|\mathcal{V}(P)| == 1$  then
13             return  $P$  /* Found the minimal NAP */

```

Algorithm 2: COARSEN

Input: The neural network N
Output: A minimal NAP specification P

```

1 Function Coarsen( $N$ )
2    $P \leftarrow \tilde{\mathcal{A}}(N)$ 
3   if  $\mathcal{V}(P) == 0$  then
4     return None; /* Return None if the most refined NAP fails verification */
5   else
6     for  $N_{i,l}$  in  $N$  do
7        $P \leftarrow \tilde{\Delta}(N_{i,l})$ ; /* Try to abstract this neuron using  $\tilde{\Delta}$  */
8       if  $\mathcal{V}(P) == 0$  then
9          $P \leftarrow \tilde{\Delta}(N_{i,l})$ ; /* Refine the neuron back if the verification fails */
10    return  $P$ ;

```

3.3 The Coarsen Approach

In contrast to the REFINE approach, the COARSEN approach starts from the most refined NAP and then gradually coarsens it. We first check if the problem is well-defined by verifying if the most

refined NAP \tilde{P} succeeds in verification. Then, for each neuron, we attempt to coarsen it using \mathcal{A} ; if the resulting NAP no longer verifies the query, we refine it back using $\tilde{\mathcal{A}}$; otherwise, we keep the coarsened NAP. We describe the above procedure in Algorithm 2. The algorithm could require $|N|$ calls to \mathcal{V} in the worst case, as proven in Theorem 3.3. Please refer to the proof in Appendix A.

Theorem 3.3. *The algorithm COARSEN returns a minimal NAP specification with $O(|N|)$ calls to \mathcal{V} .*

4 VERIFICATION FREE APPROACHES

While the REFINE and COARSEN algorithms can find minimal NAP specifications with correctness guarantees, their inefficiency poses challenges with the verification of large neural networks. To address this issue, we introduce two efficient approaches for estimating minimal NAP specifications without requiring expensive calls to the verification tool. Unlike verification-based approaches, these estimation methods are deeply linked to mandatory neurons, a key concept in dissecting the minimal NAP specification problem, as discussed below.

Definition 4.1 (Mandatory neuron). A neuron $N_{i,l} \in N$ is considered mandatory if it cannot be coarsened to $*$ in any minimal NAP specification. We denote the set of all mandatory neurons as M , defined by:

$$M = \{N_{i,l} \mid P_{i,l} \in \{\mathbf{0}, \mathbf{1}\}, P \text{ is minimal}\}$$

Note that M is the union of the set of mandatory neurons from all minimal NAP specifications. It follows that $|M| \geq s$, where s denotes the size of the largest minimal NAP specification.

The minimal NAP specification problem can be solved trivially if we gain access to M . Thus, our verification-free approaches are designed to determine mandatory neurons and estimate M . To better understand these our approaches, we first discuss the properties of mandatory neurons. Recall that verifying a robustness query given a NAP specification P is equivalent to showing that $F(x) \geq 0$ for input x in region R_P . Thus, the necessary conditions of a mandatory neuron $N_{i,l}$ can be written as follows:

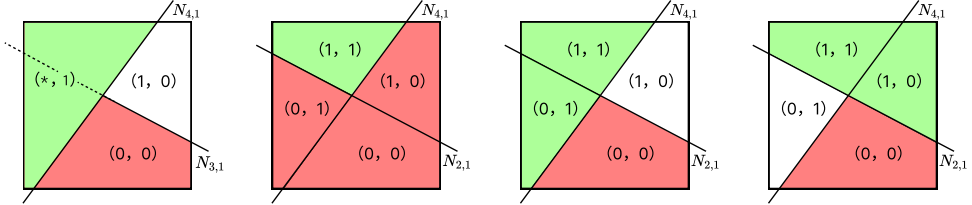
- (1) If $N_{i,l}$ is in state $\mathbf{0}$, it implies when $\hat{z}_i^{(l)}(x) = 0, F(x) \geq 0$. In addition, $\exists x$ s.t. $\hat{z}_i^{(l)}(x) > 0, F(x) < 0$.
- (2) If $N_{i,l}$ is in state $\mathbf{1}$, it implies $\forall x$ s.t. $\hat{z}_i^{(l)}(x) > 0, F(x) \geq 0$. In addition, when $\hat{z}_i^{(l)}(x) = 0, F(x) < 0$.

As for non-mandatory neurons in P , since they can be coarsened to $*$, it implies $F(x) \geq 0$ regardless of the value of $\hat{z}_i^{(l)}(x)$. Formally, this can be written as: If $N_{i,l}$ is in state $\mathbf{0}$ or $\mathbf{1}$, it implies that $\forall x, F(x) \geq 0$. In our current approaches, including the REFINE and COARSEN algorithms, we rely on interaction with the verification tool \mathcal{V} to identify mandatory neurons. Since calls to \mathcal{V} are typically computationally expensive, it would be advantageous to estimate M in a more cost-effective manner. This motivates us to study the following two verification-free approaches.

4.1 Adversarial-guided Prune

We first introduce ADVERSARIAL_PRUNE to identify mandatory neurons. Intuitively, it attempts to show a neuron $N_{i,l}$ is mandatory by providing an adversarial example x' exists.

When an adversarial example x' is found, it immediately indicates that the NAP $\mathcal{A}(N, x')$ fails the verification, i.e., $\mathcal{V}(\mathcal{A}(N, x')) = 0$. Moreover, it also implies that any NAP subsumed by $\mathcal{A}(N, x')$ fails verification. For instance, suppose an adversarial example x' is found for a simple one-layer four-neuron neural network and $\mathcal{A}(N, x')$ is $\langle \mathbf{1}, \mathbf{0}, \mathbf{1}, \mathbf{0} \rangle$. We can infer that NAPs like $\langle \mathbf{1}, \mathbf{0}, *, * \rangle$, $\langle \mathbf{1}, \mathbf{0}, *, * \rangle$, $\langle \mathbf{1}, *, *, \mathbf{0} \rangle$, and $\langle \mathbf{1}, \mathbf{0}, *, \mathbf{0} \rangle$ fail the verification. This information is particularly useful when determining if a neuron is mandatory. For example, if we know that NAP $P := \langle \mathbf{1}, \mathbf{0}, *, \mathbf{1} \rangle$ is a



(a) $N_{4,1}$ is mandatory. (b) $N_{4,1}, N_{2,1}$ are mandatory. (c) $N_{4,1}$ is mandatory. (d) $N_{2,1}$ is mandatory.

Fig. 5. Geometric interpretation of NAPs on mandatory neurons. The first subfigure represents the case when the two NAPs disagree on $N_{4,1}$. The other three subfigures represent the three cases when the two NAPs disagree on $N_{4,1}$, $N_{2,1}$. Regions colored green pass verification, whereas red indicates an adversarial example exists. Here, we omit states for $N_{1,1}$, $N_{3,1}$ in those NAPs for simplicity.

specification, i.e., $\mathcal{V}(P) = 1$, then we can easily deduce that the fourth neuron $N_{4,1}$ is mandatory. This is because that coarsening the fourth neuron would expand P to $\langle 1, 0, *, * \rangle$, which would include the adversarial example x' and thus fail the verification, as illustrated in Figure 5a. It is evident that the neuron where P and $\mathcal{A}(N, x')$ disagrees must be mandatory.

However, when the two NAPs disagree on multiple neurons, things become a little bit different. Suppose the NAP specification P is $\langle 1, 1, *, 1 \rangle$, i.e., $\mathcal{V}(\langle 1, 1, *, 1 \rangle) = 1$. We know $\mathcal{V}(\langle 1, 0, *, 0 \rangle) = 0$ by the adversarial example x' . In this case, if we coarsen the second and fourth neurons, $N_{2,1}$ and $N_{4,1}$, the NAP specification will expand to $\langle 1, *, *, * \rangle$, which will cover the $\langle 1, 0, *, 0 \rangle$, thus failing the verification. In this case, $N_{2,1}$ and $N_{4,1}$ could both be mandatory neurons or either one of them is mandatory, as illustrated in Figures 5b, 5c, 5d. So, we simply let $\{N_{2,1}, N_{4,1}\}$ be the upper bound of mandatory neurons (learned from x'). Formally, given a NAP P , we say a neuron $N_{i,l}$ is in the upper bound of mandatory neurons M if satisfies the following condition:

- (1) $N_{i,l}$ must be in the binary states, i.e., $P_{i,l} \in \{0, 1\}$
- (2) There exists x' such that $\mathcal{A}(N_{i,l}, x')$ XORs with $P_{i,l}$, i.e., $\exists x' \text{ such that } \mathcal{A}(N_{i,l}, x') \oplus P_{i,l} = 1$

Algorithm 3: ADVERSARIAL_PRUNE

Input: The neural network N , the input dataset X

Output: A collection of mandatory neurons

1 Function *Adversarial_Prune(N, X)*

2 | $Mand \leftarrow \emptyset ; P \leftarrow \tilde{\mathcal{A}}(N)$

3 **for** x_j **in** X **do**

4 | $x'_i \leftarrow \text{Adversarial}$

5 **for** $N_{i,l}$ **in** N **do**

6 if $P_{i,l} \in \{0, 1\}$ and $\ddot{\mathcal{A}}(N_{i,l}, x)$

7 $Mand \leftarrow Mand \cup \{N_{i,1}\}$ /* Create mandatory neurons for x'_i */

8 | return *Man*

The field of adversarial attacks has been extensively studied, offering a wealth of methods that we can leverage. These approaches are usually computationally efficient, making it easy to access a large collection of adversarial examples. Therefore, we can compute the upper bound of mandatory neurons efficiently by simply taking the union of upper bounds learned for each adversarial example, as illustrated in Algorithm 3.

4.2 Gradient-guided Search

We introduce another approach called GRADIENT_SEARCH to identify mandatory neurons. Similar to ADVERSARIAL_PRUNE, GRADIENT_SEARCH avoids costly interactions with the verification tool. Instead, it leverages gradient estimations to analyze the structure of F .

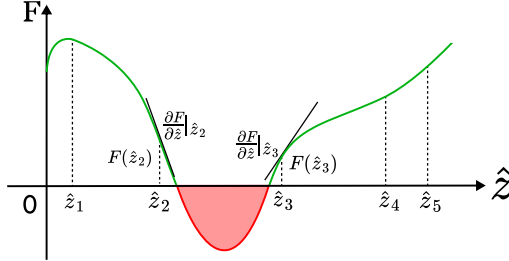


Fig. 6. The gradient provides insights into the local structure of F . When the gradient is large and the function value is small, it strongly suggests that F will go below zero nearby.

Algorithm 4: GRADIENT_SEARCH

Input: The neural network N , the input dataset X , and thresholds β, γ

Output: A collection of mandatory neurons

```

1 Function Gradient_Search( $N, X, \beta, \gamma$ )
2    $Mand \leftarrow \emptyset; P \leftarrow \tilde{\mathcal{A}}(N)$ 
3   for  $N_{i,l}$  in  $N$  do
4     for  $x_j$  in  $X$  do
5        $\hat{z}_j \leftarrow \hat{z}_i^{(l)}(x_j)$ 
6       if  $\hat{z}_j > 0$  then
7         if  $|F(\hat{z}_j)| < \beta$  and  $|\frac{\partial F}{\partial \hat{z}_i^{(l)}}|_{\hat{z}_j} > \gamma$  and  $P_{i,l} == 0$  then
8            $Mand \leftarrow Mand \cup \{N_{i,l}\}$       /* Neuron is in state 0, can't coarsen */
9         else
10        if  $F(\hat{z}_j) < 0$  and  $P_{i,l} == 1$  then
11             $Mand \leftarrow Mand \cup \{N_{i,l}\}$       /* Neuron is in state 1, can't coarsen */
12


---


return  $Mand$ 
```

Recall our definition of a neural network in Section 2.1, where the output $F(x)$ can be seen as a function of the post-activation value of any internal neuron $\hat{z}_i^{(l)}$. We denote this function as $F(\hat{z}(x))$, omitting i and l for simplicity. The function $F(\hat{z})$ is non-linear and operates within an input range of $\hat{z} \in [0, +\infty)$. It is worth noting that the gradient $\frac{\partial F}{\partial \hat{z}}$ can provide valuable insights into the local structure of F . This insight may help determine the necessity condition of mandatory neurons by checking if there exists a \hat{z} such that $F(\hat{z}) < 0$ for the corresponding neuron. To be more specific, given some sampled data $\hat{z}_1, \dots, \hat{z}_n$, we can compute their corresponding function values $F(\hat{z}_1), \dots, F(\hat{z}_n)$ along with their gradients $\frac{\partial F}{\partial \hat{z}}|_{\hat{z}_1}, \dots, \frac{\partial F}{\partial \hat{z}}|_{\hat{z}_n}$. Then if there exists a \hat{z}_j such that $|F(\hat{z}_j)|$ is sufficiently small, yet the norm of its gradient $|\frac{\partial F}{\partial \hat{z}}|_{\hat{z}_j}$ is significantly large, then it is very likely that F will go below zero nearby, as illustrated in Figure 6. Then, if we happen to know that the corresponding neuron $N_{i,l}$ is in state 0, it is highly likely that $N_{i,l}$ is mandatory. Conversely, if a neuron $N_{i,l}$ is in state 1, and we sample an x such that $\hat{z}_i^{(l)} = 0$ and $F(x) < 0$, we immediately

recognize that the neuron is mandatory. Algorithm 4 presents pseudocode for estimating whether a neuron is mandatory based on the discussions above.

Both the estimation method GRADIENT_SEARCH and ADVERSARIAL_PRUNE can be used together. Taking the intersection of their estimated results may provide us with a better overall estimate. In addition, the estimated mandatory neurons can serve as an initial starting point in our statistical versions of the REFINE and COARSEN approaches introduced in Section 5.

Our experimental results regarding these two estimation approaches indicate a notable trend: neurons from deeper layers are more likely to be mandatory. This observation aligns with commonly-held beliefs that deeper neurons are generally linked to high-level feature representation, and thus play a more important role than shallow neurons in final classification decisions. This observation leads us to a valuable heuristic: prioritizing deeper neurons over shallower ones as we iterate through neurons in our implementations of the REFINE and COARSEN algorithms.

5 STATISTICAL LEARNING APPROACHES

In this section, we introduce two new algorithms that address the minimal NAP specification problem. While they share the same overarching concept as REFINE and COARSEN, these methods employ sampling and statistical learning principles to efficiently learn a minimal NAP specification. Recall that the set of mandatory neurons M is the union of all neurons that appears in any minimal specification and is an upper bound of the largest minimal specification.

5.1 The Statistical Refine Approach

Mandatory neurons are crucial for forming NAP specifications, as their binary states play a critical role in determining the neural network's robustness performance. We leverages this property to find mandatory neurons statistically. To be more specific, suppose we sample some NAPs P_1, P_2, \dots, P_n from the NAP family \mathcal{P} . For those NAPs that qualify as specifications (i.e., $\mathcal{V}(P) = 1$), mandatory neurons should appear more frequently in them than in those NAPs that fail the verification tool (i.e., $\mathcal{V}(P) = 0$).

Based on this insight, we propose an approach called SAMPLE_REFINE that relies on non-repetitive sampling to identify mandatory neurons for solving the minimal NAP problem. We start with the coarsest NAP and iteratively collect the most probable mandatory neurons. In every iteration, we sample k NAPs by refining unvisited neurons with some probability θ . The sampled NAPs are then fed to the verification tool, and the neuron that appears most frequently in verifiable NAPs is the most probable mandatory neuron in this iteration. The neuron is marked as visited, and the process stops when either we collect s neurons (assuming that s is known), or the current mandatory neurons form a NAP specification P , i.e., $\mathcal{V}(P) = 1$. Finally, we return the learned NAP, obtained by applying \mathcal{A} to the collected neurons. The algorithm 5 provides an overview of the above procedure.

It is worth noting that SAMPLE_REFINE doesn't guarantee correctness, as we may end up collecting only the s most probable mandatory neurons, which may not be sufficient to form a specification. Another concern regarding this algorithm is sampling efficiency, specifically the potential for the number of samples required to grow exponentially with the size of the minimal NAP specification s . To understand why this is problematic, consider a scenario where the only minimal NAP specification P consists of all mandatory neurons; in this case, all $|M|$ neurons must be selected for P to be learned. If θ is set to a constant value, then the expected number of samples needed to obtain the NAP specification is $(\frac{1}{\theta})^{|M|}$. To address this, we set $\theta = \left(\frac{|M|}{|M|+1}\right)^{|M|}$. This choice ensures that the sampling efficiency is polynomial in both $|M|$ and s , as proven in Theorem 5.1. Please refer

to the proof in the Appendix B. In addition, Theorem 5.1 also shows that with high probability, a mandatory neuron will be found with $O(\log|N|)$ calls to \mathcal{V} .

Algorithm 5: SAMPLE_REFINE

Input: The neural network N , the probability θ , sample size k , and the size s
Output: A minimal NAP specification P

```

1 Function Sample_NAPs(unvisited, θ)
2    $P \leftarrow \mathcal{A}(N)$                                 /* Use the coarsest NAP as a blank template */
3   for  $N_{i,l}$  in unvisited do
4      $rand \leftarrow \text{random}(0, 1)$ 
5     if  $rand \leq \theta$  then
6        $P \leftarrow \tilde{\Delta}(N_{i,l})$           /* Refine unvisited neurons using  $\tilde{\Delta}$  with probability  $\theta$  */
7   return  $P$ 

8 Function Sample_Refine(visited, θ, k, s)
9   while  $|\text{visited}| < s$  and  $\mathcal{V}(P) == 0$  do
10     $unvisited \leftarrow N \setminus \text{visited}$ 
11     $ctr = \text{dict}()$                                 /* Create a counter for each neuron in unvisited */
12    for  $_$  in range( $k$ ) do
13       $P \leftarrow \text{Sample\_NAPs}(unvisited, \theta)$           /* Sample  $k$  NAPs */
14      for  $N_{i,l}$  in unvisited do
15        if  $P_{i,l} == \tilde{\mathcal{A}}(N_{i,l})$  and  $\mathcal{V}(P) == 1$  then
16           $ctr[N_{i,l}] += 1$                          /* Count successful NAPs for each neuron */
17     $N_{\text{mad}} \leftarrow \text{argmax}_{N_{i,l} \in \text{unvisited}} \{ctr[N_{i,l}]\}$       /* Pick potential mandatory neuron */
18     $visited \leftarrow \text{visited} \cup \{N_{\text{mad}}\}$ 
19  return  $\tilde{\mathcal{A}}(visited)$ 

20  $P \leftarrow \tilde{\mathcal{A}}(N)$ 
21 if  $\mathcal{V}(P) == 0$  then
22   return None                                /* Return None if the most refined NAP fails verification */
23 else
24   if heuristics then
25      $visited \leftarrow \text{Gradient\_Search}(N) \cap \text{Adversarial\_Prune}(N)$ 
26   else
27      $visited \leftarrow \emptyset$                       /* Start from the coarsest NAP */
28   Sample_Refine(visited, θ, k, s)

```

Theorem 5.1. *With probability $\theta = |(\frac{|M|}{|M|+1})|^{M|}$, SAMPLE_REFINE has $1 - \delta$ probability of outputting a minimal NAP specification with $\Theta(|M|^2(\log|N| + \log(s/\delta)))$ examples each iteration and $O(s|M|^2(\log|N| + \log(s/\delta)))$ total calls to \mathcal{V} .*

5.2 The Statistical Coarsen Approach

The COARSEN algorithm begins with the most refined NAP and progressively coarsens each neuron until the verification process fails. Enhancing the algorithm's performance is possible by coarsening multiple neurons during each iteration. However, a fundamental question emerges: How do we determine which set of neurons to coarsen in each round?

We present SAMPLE_COARSEN to answer this question. In this approach, we assume that each neuron is independent of the others and select neurons to coarsen in a statistical manner. Specifically, in each iteration, we randomly coarsen a subset of refined neurons in the current NAP

simultaneously to see if the new NAP can pass verification. We repeat this process until the NAP size reaches s . Algorithm 6 provides the pseudocode for SAMPLE_COARSEN.

Similar to SAMPLE_REFINE, SAMPLE_COARSEN also faces the same challenge related to sample efficiency. To better illustrate this, suppose a minimal NAP specification P with size s can be found after one iteration of refinement. Then, the probability of selecting the exact number of s mandatory neurons in P is θ^s . Consequently, if θ is set to a constant value, the expected number of samples needed to find the NAP is $(\frac{1}{\theta})^s$. Unlike SAMPLE_REFINE, we know the refinement will always ensure the resulting NAP can pass verification. So, once such a NAP is learned, we can narrow down the estimated mandatory neurons by an expected factor of θ . In this way, the expected number of samples and the expected number of iterations are inversely related, yet their product is the total number of calls to \mathcal{V} . We demonstrate that by setting $\theta = e^{-\frac{1}{s}}$, we not only make the expected number of samples polynomial in s , but also minimize the total number of calls to \mathcal{V} , as proven in Theorem 5.2. Please refer to the proof in Appendix B.

Theorem 5.2. *With probability $\theta = e^{-\frac{1}{s}}$, SAMPLE_COARSEN learns a minimal NAP specification with $\mathcal{O}(s \log |N|)$ calls to \mathcal{V} .*

Algorithm 6: SAMPLE_COARSEN

Input: The neural network N , the probability θ , and the size s
Output: A minimal NAP specification P

```

1 Function Sample_Coarsen(mand_neurons,  $\theta$ ,  $s$ )
2    $P \leftarrow \tilde{\mathcal{A}}(N)$ ; mand_neurons  $\leftarrow N$ 
3   if  $\mathcal{V}(P) == 0$  then
4     return None      /* Return None if the most refined NAP fails verification */
5   else
6     while  $|P| > s$  do
7        $P \leftarrow \text{Sample\_NAPs}(\text{mand\_neurons}, \theta)$ 
8       if  $\mathcal{V}(P) == 1$  then
9         found_neurons  $\leftarrow \emptyset$ 
10        for  $N_{i,l}$  in  $N$  do
11          if  $P_{i,l} == \tilde{\mathcal{A}}(N_{i,l})$  then
12            found_neurons  $\leftarrow \text{found\_neurons} \cup \{N_{i,l}\}$ 
13            mand_neurons  $\leftarrow \text{found\_neurons}$           /* Reduce search space */
14          else
15             $P \leftarrow \text{Sample\_Naps}(\text{mand\_neurons}, \theta)$           /* Sample a new NAP */
16   return  $P$           /* Return the minimal NAP of size  $s$  */

```

Setting the sample probability θ . Setting s poses a challenge in practice, as we assume that s is always provided in SAMPLE_REFINE and SAMPLE_COARSEN. However, this can be addressed by dynamically updating θ based on the result of $\mathcal{V}(P)$ [Liang et al. 2011]. With θ from theorem 5.2, SAMPLE_COARSEN finds a NAP specification with probability $(e^{-1/s})^s = e^{-1}$. Recall that theorem 5.1 state that SAMPLE_REFINE finds a NAP specification with probability $\left(\frac{|M|}{|M|+1}\right)^{|M|}$. The probability approaches e^{-1} asymptotically. Thus, we aim to set θ such that the $\Pr(\mathcal{V}(P) = 1) = e^{-1}$. Intuitively, if a sampled NAP P is a specification, we decrease θ so less neurons will be refined or more neurons will be coarsened. Similarly, if P is not a specification, θ needs to be increased.

Given that $\theta \in [0, 1]$, we can parameterize it using the Sigmoid function $\sigma(\lambda) = (1 + e^{-\lambda})^{-1}$, where $\lambda \in (-\infty, \infty)$. Since $\Pr(\mathcal{V}(P) = 1)$ depends on θ as well, we express it as a function of λ ,

$g(\lambda) = \Pr(\mathcal{V}(P) = 1)$. Then, setting $\Pr(\mathcal{V}(P) = 1) = e^{-1}$ can be achieved through the following minimization problem:

$$L(\lambda) = \frac{1}{2}(g(\lambda) - e^{-1/s})^2 \quad (12)$$

The loss function $L(\lambda)$ can be minimized by statistical learning using stochastic gradient descent. With a step size η , update λ using $\lambda \leftarrow \lambda - \eta \frac{dL}{d\lambda}$. Note that $\frac{dL}{d\lambda}$ can be expressed as:

$$\frac{dL}{d\lambda} = (g(\lambda) - e^{-1/s}) \frac{dg(\lambda)}{d\lambda} \quad (13)$$

Given $g(\lambda) = \Pr(\mathcal{V}(P) = 1)$, we can replace $g(\lambda)$ with $\mathcal{V}(P)$ for stochastic gradient update. Additionally, since $\frac{dg(\lambda)}{d\lambda} > 0$, we simply ignore it as its multiplication effect can be represented by η . Therefore, the final update rule is given by:

$$\lambda \leftarrow \lambda - \eta(\mathcal{V}(P) - e^{-1}) \quad (14)$$

6 VOLUME ESTIMATION OF R_P

Conceptually, NAP specifications typically correspond to significantly larger input regions compared to local neighbourhood specifications. This serves as the primary motivation for utilizing NAPs as specifications. However, previous work lacks sufficient justification or evidence to support this claim. In this section, we propose a simple method for approximating the volume of R_P , i.e., the region corresponding to a NAP P . This allows us to: 1) quantify the size difference between R_P and L_∞ ball specifications; 2) gain insights into the volumetric change from the most refined NAP specification to the minimal NAP specification.

Computing the exact volume of R_P is at least NP-hard, as determining the exact volume of a polygon is known to be NP-hard [Dyer and Frieze 1988]. Moreover, computing the exact volume of R_P can be even more challenging due to its potential concavity. To this end, our method estimates the volume of R_P by efficient computation of an orthotope that closely aligns with R_P , as illustrated in Figure 7. We briefly describe it as follows:

Finding an anchor point. The first step is to find an anchor point to serve as the center of the orthotope. Ideally, this anchor point should be positioned close to the center of R_P to ensure a significant overlap between the orthotope and R_P . However, computing the actual center of R_P is costly. Thus, we look for a pseudo-center from the training set X that resides in R_P . This pseudo-center can be computed by finding the point that uses the smallest L_∞ ball to cover other data points, solved as the following optimization problem:

$$c_{\text{pseudo}} = \arg \min_{x \in R_P} \max_{x' \in R_P} \|x - x'\|_\infty$$

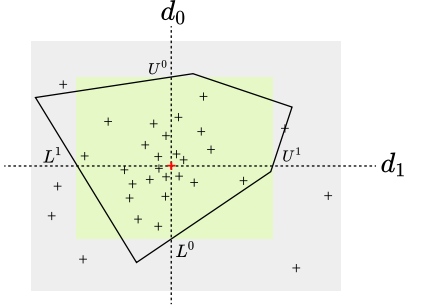


Fig. 7. Volume Estimation of R_P using an orthotope in a 2-dimensional case. The gray rectangle represents the input space, with the training set depicted by a collection of data points $+$. The polygon corresponds to some NAP P . Initially, we identify an anchor point, denoted by $+$. Then, we construct the orthotope, represented by the green rectangle, by extending upper and lower bounds starting from the anchor point until it extends beyond P .

where $R_P = \{x \mid \mathcal{A}(N, x) \leq P, x \in X\}$. When $|X|$ is small, c_{pseudo} can be computed directly; for larger $|X|$, a statistical computation strategy is required.

Constructing the orthotope. Once the pseudo-center c_{pseudo} is determined, we want to create an orthotope around c_{pseudo} to closely align with R_P . The orthotope is constructed by determining pairs of upper and lower bounds $U^{(i)}$ and $L^{(i)}$ for each dimension i . Specifically, $U^{(i)}$ and $L^{(i)}$ are computed through expansion in two opposite directions from c_{pseudo} along dimension i until they extend beyond R_P . This expansion can be expressed as:

$$\max_{U^{(i)}} \{x' \in R_P \mid x' := c_{\text{pseudo}} + U^{(i)}\} ; \max_{L^{(i)}} \{x' \in R_P \mid x' := c_{\text{pseudo}} - L^{(i)}\}$$

Here, $U^{(i)}$ and $L^{(i)}$ represent the upper and lower bounds in dimension i respectively, originating from c_{pseudo} . These bounds can be efficiently calculated with binary search.

The choice of the archer point is crucial in our approach. If it is located at a corner of R_P , the volume calculation will be highly biased. This can pose a problem when we seek to understand the volumetric change from the most refined NAP specification to the minimal NAP specification. Additionally, using the orthotope as an estimator provides convenience in understanding the volumetric change simply by examining differences in each input dimension.

7 EVALUATION

In this section, we conduct a comprehensive evaluation of our algorithms for learning minimal NAP specifications across a range of benchmarks, spanning from a simple binary classifier to the state-of-the-art image classification model. To align with the underlying verification engine in the Experiment Setup, we evaluate NAP with ReLU as activation function. To illustrate the effectiveness of our approaches, we chose the method proposed in [Geng et al. 2023] as the baseline, denoted as the $\tilde{\mathcal{A}}$ function. Our results suggest that minimal NAP specifications typically involve only a fraction of the neurons compared to the most refined NAPs (calculated using the $\tilde{\mathcal{A}}$ function), yet they dramatically extend the verifiable bounds by several orders of magnitude.

Experiment Setup. All experiments in this section were conducted on an Ubuntu 20.04 LTS machine with 172 GB of RAM and an Intel(R) Xeon(R) Silver Processor. For verification, we utilized Marabou [Katz et al. 2019], a dedicated state-of-the-art neural network verifier. We configured a timeout of 10 minutes for each call to the verification tool. If the timeout is exceeded, the current neuron is retained in the minimal NAP specification even if its status cannot be determined.

Table 1. Overview of the size of learned minimal NAP specifications using various approaches on the WBC benchmark. The columns represent different labels, while each row corresponds to a different algorithm. $|P|$ denotes the size of the learned NAP, and $\#\mathcal{V}$ represents the number of calls to \mathcal{V} ("—" indicates not applicable). The remaining columns, train and test, report the percentile (%) of train and test data covered by P .

| | 0 | | | | 1 | | | |
|------------------------------------|-------|-----------------|-------|-------|-------|-----------------|-------|-------|
| | $ P $ | $\#\mathcal{V}$ | train | test | $ P $ | $\#\mathcal{V}$ | train | test |
| The $\tilde{\mathcal{A}}$ function | 102 | - | 78.11 | 81.40 | 93 | - | 87.06 | 80.28 |
| COARSEN | 31 | 102 | 98.22 | 95.35 | 32 | 93 | 99.65 | 94.37 |
| ADVERSARIAL_PRUNE | 61 | - | 81.06 | 88.37 | 54 | - | 87.06 | 80.28 |
| GRADIENT_SEARCH | 43 | - | 82.84 | 88.37 | 39 | - | 93.37 | 87.32 |
| SAMPLE_REFINE | 53 | 187 | 92.43 | 89.37 | 56 | 264 | 89.86 | 88.51 |
| SAMPLE_COARSEN | 42 | 47 | 94.69 | 92.34 | 45 | 41 | 94.15 | 91.52 |

Table 2. Overview of the size of learned minimal NAP specifications on the MNIST benchmark.

| | 0 | | | | 1 | | | | 4 | | | |
|------------------------------------|-------|-----------------|-------|-------|-------|-----------------|-------|-------|-------|-----------------|-------|-------|
| | $ P $ | $\#\mathcal{V}$ | train | test | $ P $ | $\#\mathcal{V}$ | train | test | $ P $ | $\#\mathcal{V}$ | train | test |
| The $\tilde{\mathcal{A}}$ function | 751 | - | 79.50 | 80.51 | 745 | - | 86.01 | 85.11 | 712 | - | 77.54 | 80.24 |
| COARSEN | 480 | 751 | 98.68 | 98.78 | 491 | 745 | 98.90 | 98.59 | 506 | 712 | 98.51 | 97.45 |
| ADVERSARIAL_PRUNE | 618 | - | 83.13 | 71.32 | 630 | - | 79.02 | 76.51 | 699 | - | 82.66 | 84.12 |
| GRADIENT_SEARCH | 195 | - | 92.1 | 91.80 | 237 | - | 89.73 | 88.39 | 169 | - | 87.59 | 88.51 |
| SAMPLE_REFINE | 564 | 4059 | 90.03 | 87.91 | 570 | 3663 | 88.36 | 86.84 | 581 | 4532 | 82.90 | 83.46 |
| SAMPLE_COARSEN | 532 | 33 | 93.19 | 93.01 | 559 | 27 | 94.12 | 93.68 | 562 | 25 | 93.89 | 93.64 |

7.1 Wisconsin Breast Cancer with Binary Classifier

We conduct our first experiment using a four-layer neural network as a binary classifier, where each layer consists of 32 neurons. This classifier is trained on the Wisconsin Breast Cancer (WBC) dataset [Wolberg et al. 1995], representing a decision-critical task where robustness is essential. Our trained model achieves a test set accuracy of 95.61%. We calculate the most refined (baseline) NAP specifications \tilde{P}^0 and \tilde{P}^1 for labels 0 and 1 using the statistical abstraction function $\tilde{\mathcal{A}}$ with a confidence ratio of $\delta = 0.95$. The size of \tilde{P}^0 and \tilde{P}^1 are 102 and 93, respectively. In contrast, the sizes of the minimal NAP specifications learned by the COARSEN algorithm for labels 0 and 1 are significantly reduced to 31 and 32, respectively. It is worth mentioning that our estimation approaches provide a fairly accurate estimate of the mandatory neurons, despite computing rather loose upper bounds. To be more specific, ADVERSARIAL_PRUNE and GRADIENT_SEARCH compute 61 and 43 mandatory neurons for label 0, respectively. Together, they cover 25 out of the 31 mandatory neurons appearing in the minimal NAP specification for label 0. For label 1, ADVERSARIAL_PRUNE and GRADIENT_SEARCH compute 54 and 39 mandatory neurons, respectively, covering 25 out of the 32 mandatory neurons appearing in the minimal NAP specification for label 1.

Regarding the statistical approaches, SAMPLE_REFINE computes NAP specifications of size 53 and 56 for label 0 and label 1, respectively. This is achieved while making 187 and 264 calls, respectively. Although these numbers are quite large, it is expected since it has to sample multiple trials in each iteration. In contrast, SAMPLE_COARSEN is significantly more efficient. It can learn NAP specifications of size 42 and 45 for label 0 and label 1 using only 47 and 41 calls, respectively.

Recall that one of the main motivations for learning the minimal NAP specifications is their potential to verify larger input regions compared to refined NAP specifications. To support this, we compute the percentile of unseen test data that can be verified using these NAPs. Test data, sampled from the input space, serve as a proxy to understand the verifiable bounds of different NAPs. We find that the most refined NAP specifications \tilde{P}^0 and \tilde{P}^1 cover 81.40% and 80.28% of test data for labels 0 and 1, respectively. In contrast, minimal NAP specifications cover 95.35% and 94.37% of test data for labels 0 and 1, respectively.

To intuitively understand the change in verifiable regions R_P from refined to minimal NAP specifications, we compare their estimated volumes. The increase in estimated volume is substantial: 58324.35 times larger for label 0 and 3053.53 times larger for label 1. Figure 8 illustrates the comparison of verifiable input ranges between the refined and minimal NAP specifications for labels 0 and 1, referencing the anchor point.

7.2 MNIST with Fully Connected Network

To show that our insights and approaches can be applied to more complicated datasets and networks, we conduct the second set of experiments using the `mnistfc_256x4` model [VNNCOMP 2021], a

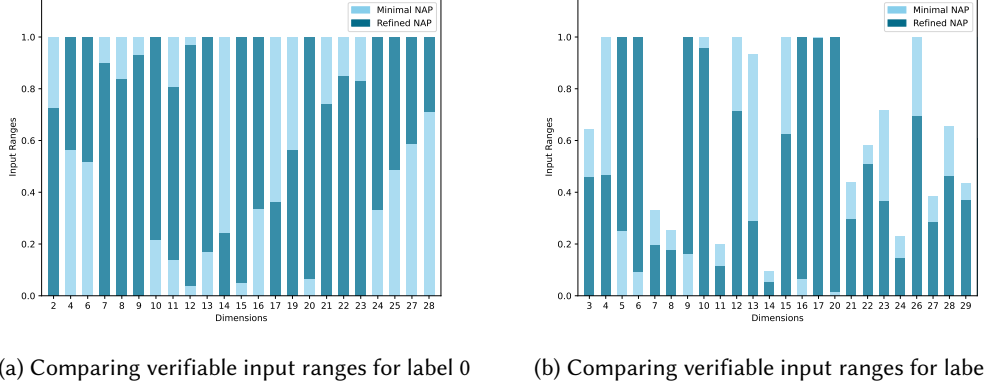


Fig. 8. Comparison of verifiable input ranges between the refined NAP specifications and the minimal NAP specifications for labels 0 and 1 on the Wisconsin Breast Cancer dataset, with reference to the anchor point. The minimal NAP specifications enable verification over a larger input range for all dimensions.

4-layer fully connected network with 256 neurons per layer trained on the MNIST dataset. We specifically focus on classes 0, 1, and 4, as evaluations on other labels either encounter timeouts or fail verification. We compute the most refined NAP specifications \tilde{P}^0 , \tilde{P}^1 , and \tilde{P}^4 for these labels with a confidence ratio of $\delta = 0.99$. Their sizes are 751, 745, and 712, respectively, consistent with baseline results from previous work.

In contrast, the minimal NAP specifications learned by the COARSEN algorithm for labels 0, 1, and 4 are significantly reduced to 480, 491, and 506, respectively. Notably, our estimation approaches accurately identify mandatory neurons in these minimal NAPs. For example, for label 0, ADVERSARIAL_PRUNE and GRADIENT_SEARCH find 618 and 195 mandatory neurons, respectively, and discover 445 and 160 of the 480 mandatory neurons in the minimal NAP specification.

In terms of statistical approaches, SAMPLE_COARSEN outperforms SAMPLE_REFINE in both NAP specification size and number of calls to \mathcal{V} , requiring around 30 calls compared to over 3000. It's interesting to note that the mandatory neurons presented in the learned minimal NAP specifications using different algorithms are mostly located in the 3rd and 4th layers. This aligns with the belief that neurons in deeper layers are responsible for high-level feature representation and thus play a critical role in making classification decisions.

Moreover, the learned minimal NAP specifications correspond to significantly larger verifiable regions compared to the refined NAP specifications. Using the percentile of test data as a metric, the minimal NAP specifications increase the coverage ratio from 80.51% to 98.78%, 85.11% to 98.59%, and 80.24% to 97.45% for labels 0, 1, and 4, respectively. From the perspective of estimated volume, the volumetric changes are on the order of 10^8 times larger.

7.3 ImageNet with Deep Convolutional Neural Network

Current verification methods struggle to scale to state-of-the-art neural networks, making them unsuitable for critical systems like deep learning-based autonomous driving. Thus, our verification-dependent approaches also face scalability issues. We evaluate our learnt minimal specification using verification free approaches, an aspect not well-studied in the current literature.

Thus, for the third experiment, we choose a deep convolutional network, specifically a pretrained VGG-19 for ImageNet dataset, as the benchmark for estimating mandatory neurons. We select

Table 3. Overview of the size of learned minimal NAP specifications on the ImageNet benchmark.

| | box_turtle | labrador_retriever | acorn_squash | confectionery | stone_wall | | | |
|------------------------------------|------------|--------------------|--------------|---------------|------------|-------|-------|-------|
| | $ P $ | test | $ P $ | test | $ P $ | test | $ P $ | test |
| The $\tilde{\mathcal{A}}$ function | 1978 | 39.42 | 691 | 39.61 | 1003 | 29.23 | 878 | 33.84 |
| ADVERSARIAL_PRUNE | 1863 | 39.42 | 661 | 41.28 | 823 | 25.68 | 845 | 23.07 |
| GRADIENT_SEARCH | 611 | 53.30 | 572 | 87.01 | 301 | 52.40 | 256 | 44.23 |
| | | | | | | | 260 | 54.90 |

neurons from fully connected layers¹ of VGG-19, which contains a total of 8192 neurons, to compute NAPs. The original ImageNet includes 1000 classes with millions of images. We narrow our focus to the top five largest classes in ImageNet. Each class consists of around 1000 training images and 350 test images. Table 3 presents the results of the learned NAPs using verification-free approaches.

We observe that these estimated NAPs cover significant portions of unseen test data. For example, the NAP formed by mandatory neurons learned through GRADIENT_SEARCH can cover 87.01% of test data. This makes them a promising candidate for serving as NAP specifications, which tend to generalize well to unseen data drawn from the underlying distribution.

NAP Captures Visual Interpretability and Inherent Robustness. From the perspective of representation learning, neural networks acquire both low- and high-level feature extractors, which they use to make final classification decisions based on hidden features (neuron representations) [Bengio et al. 2013]. Therefore, the robustness and consistency of a model’s predictions are influenced by the quality of these learned features. In essence, achieving an accurate and robust model hinges on learning “good” hidden representations, which are characterized by better interpretability [Zhang et al. 2021]. Many studies suggest a close relationship between visual interpretability and robustness, often observed in the learned features and representations [Alvarez Melis and Jaakkola 2018; Boopathy et al. 2020; Dong et al. 2017]. Thus, although we cannot yet formally verify the correctness of these estimated NAP specifications, we demonstrate that these NAPs are indeed “meaningful” through visual interpretability—strong evidence that the estimated mandatory neurons (NAPs) contribute to the model’s robustness.

To this end, we employ Grad-CAM [Selvaraju et al. 2017], a popular approach from the model interpretability domain. This technique leverages the gradients of the classification score with respect to the final convolutional feature map to highlight the most important regions of an input image. Formally, the class-discriminative localization map (Grad-CAM map) $L_{\text{Grad-CAM}}^c \in \mathbb{R}^{u \times v}$ of width u and height v for any class c can be computed by:

$$L_{\text{Grad-CAM}}^c = \text{ReLU} \left(\sum_k \alpha_{c,k} A_k \right)$$

where A_k is a feature map and $\alpha_{c,k}$ is a weight which represents the significance of A_k for class c . $\alpha_{c,k}$ can be computed by:

$$\alpha_{c,k} = \frac{1}{Z} \sum_i \sum_j \frac{\partial y_c}{\partial A_{k,ij}}$$

where $\frac{\partial y_c}{\partial A_k}$ represents the gradient of the score y_c for class c with respect to the activations A_k of a convolutional layer. These gradients are globally average-pooled to obtain $\alpha_{c,k}$. To investigate whether the estimated NAPs (mandatory neurons) are related to visual interpretability, we perform a simple modification to Grad-CAM: we mask out the neurons that do not appear in NAP P using a mask M_P in the fully connected layers. We then calculate the backward gradient flow based on the

¹We leave NAP computation for other layers such as convolutional layers for future work.

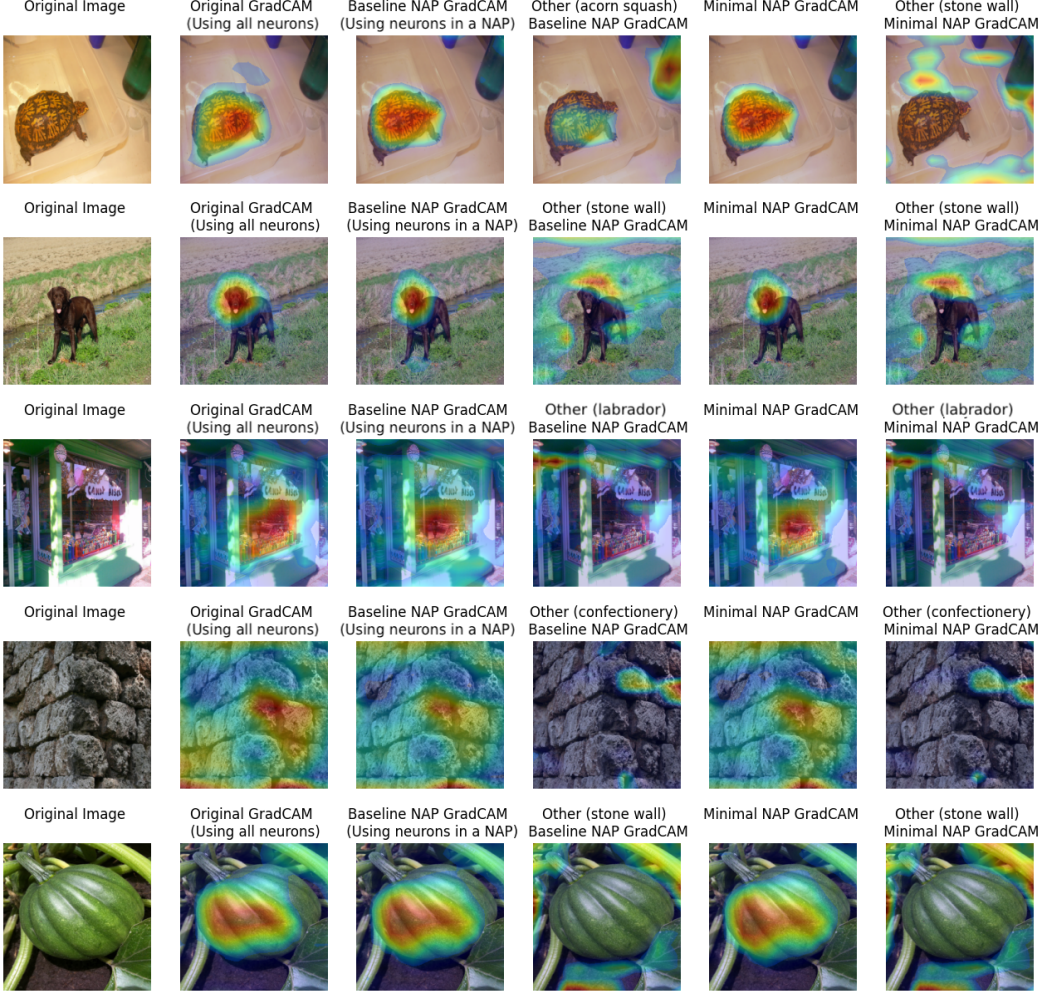


Fig. 9. Visual interpretability of learned hidden representations retained by estimated NAPs. The first two columns represent the original images and GradCams, respectively. The third and fourth columns represent modified GradCams using baseline NAPs of the same class and another class, respectively. The last two columns represent modified GradCams using minimal NAPs of the same class and another class, respectively.

modified computation graph, denoted as $\frac{\partial y_c}{\partial A_{k,ij}} M_P$. By replacing $\frac{\partial y_c}{\partial A_{k,ij}}$ with $\frac{\partial y_c}{\partial A_{k,ij}} M_P$, we compute the modified Grad-CAM map. Finally, we conduct the following experiments on image samples:

- (1) Calculate the modified Grad-CAM map using the most refined (baseline) NAP and compare it with the original Grad-CAM map.
- (2) Calculate the modified Grad-CAM map using NAPs estimated by `ADVERSARIAL_PRUNE` and `GRADIENT_SEARCH`, and compare it with the original map.
- (3) Calculate the modified Grad-CAM map using NAPs from different classes and compare it with the original map.

Figure 9 presents the experimental results. The original GradCams highlight important regions of images corresponding to crucial justifications for classification. Notably, both the most refined

NAPs and the estimated minimal NAPs highlight regions nearly identical to the original GradCams. This indicates that although the neuron abstractions learned from our minimal specification only consist of a very small fraction of neurons, they preserve the essential visual features. This suggests that the estimated minimal NAPs capture salient traces of the internal decision-making process of VGG-19, aligning with the "NAP robustness property." Additionally, GradCAMs generated using NAPs from different classes highlighted distinct regions. This strongly suggests that our estimated NAPs are distinguishable from each other, aligning with "the non-ambiguity property".

This study demonstrates that NAPs hold significant value in interpretability. A small subset of neurons from NAPs can categorize critical internal dynamics of neural networks, potentially helping us unveil the black-box nature of these systems. From a machine-checkable definition perspective, concise NAPs are easier to decode into human-understandable programs than more refined NAPs. This underscores the importance of learning minimal NAPs. Interpreting NAPs into human-readable formats remains a direction for future research.

NAP as a Defense Against Adversarial Attacks. From a practical point of view, we believe that even before 1) formal verification finally scales; and/or 2) NAPs are fully interpretable, NAPs, as they are now, can already serve as an empirical certificate of a prediction or some defense mechanism, as shown in recent work [Lukina et al. 2021]. In the same spirit, we demonstrate that our estimated essential neurons can serve as defense against adversarial attacks.

We first select images that meet two criteria: 1) correctly predicted by the model; and 2) covered by the respective NAP. On average, each NAP covers approximately 40% of the training data of the corresponding class. For each selected image, we generate 100 distinct adversarial examples that are misclassified by the model, using Projected Gradient Descent attack [Madry et al. 2018] and Carlini Wagner attack [Carlini and Wagner 2017] respectively. We then check whether each adversarial image's activation pattern is rejected by the respective NAPs. If so, we conclude that NAPs can empirically serve as specifications; Otherwise, they are proven to be not robust. Notably, we find that both the baseline NAPs and the estimated minimal NAPs reject all adversarial examples, indicating their effectiveness in describing a safe region and their potential as certificates.

8 RELATED WORK

8.1 Neural Network Verification

Neural network verification has attracted much attention due to the increasingly widespread applications of neural networks in safety-critical systems. It's NP-hard nature resulting from the non-convexity introduced by activation functions [Katz et al. 2017] makes it a challenging task. Thus most of the existing work on neural network verification focuses on designing scalable verification algorithms. For instance, while initially proposed solver-based approaches [Cheng et al. 2017; Ehlers 2017; Huang et al. 2017b; Tjeng et al. 2019] were limited to verify small neural networks with fewer than 100 neurons, state-of-the-art methods [Lu and Kumar 2019; Wang et al. 2021c; Xu et al. 2021] can verify more complex neural networks. It is worth mentioning that most existing work adopts local neighborhood specifications to verify the robustness properties of neural networks [Shapira et al. 2023]. Despite being a reliable measure, using specifications that define local neighborhood of reference data points may not cover any test data, let alone generalizing to the verification of unseen test set data. Geng et al. [2023] propose the new paradigm of NAP specifications to address this challenge. Our work advances the understanding of NAP specifications.

8.2 Abstract Interpretation

Abstract interpretation [Cousot and Cousot 1977] is a fundamental concept in software analysis and verification, particularly for approximating the semantics of discrete program states. By

sacrificing precision, abstract interpretation typically enables scalable and faster proof finding during verification [Cousot and Cousot 2014]. Although abstract interpretation for neural network verification has been proposed and studied in previous literature [Gehr et al. 2018; Mirman et al. 2018], abstract interpretation of neural activation patterns for verification is a relatively new field. Perhaps the most related work from the perspective of abstract interpretation is learning minimal abstractions [Liang et al. 2011]. While our work shares similarities in problem formulation and statistical approaches, we address fundamentally different problems. One limitation in our work is that our abstraction states may be too coarse: value in range $(0, +\infty)$ is abstracted into one state. This approach could over-approximate neuron behavior and thus fail to prove certain properties. We observe that neuron values exhibit different patterns in range for different input classes, suggesting the potential existence of more abstraction states. We leave this as future work.

8.3 Neural Activation Patterns

Neural activation patterns have commonly been used to understand the internal decision-making process of neural networks. One popular line of research is feature visualization [Bäuerle et al. 2022; Yosinski et al. 2015], which investigates which neurons are activated or deactivated given different inputs. This is also naturally related to the field of activation maximization [Simonyan et al. 2014], which studies what kind of inputs could mostly activate certain neurons in the neural network. In this way, certain prediction outcomes may be attributed to the behavior of specific neurons, thereby increasing the interpretability of the underlying models. Lukina et al. [2021] demonstrates that neural activation patterns can be used to monitor neural networks and detect novel or unknown input classes at runtime. They provide human-level interpretability of neural network decision-making. In summary, most of existing works focus on learning statistical correlations between NAPs and inputs [Bau et al. 2017; Erhan et al. 2009], or between NAPs and prediction outcomes [Lukina et al. 2021]. However, these correlations raises questions which we address in this paper: whether the correlation can be trusted or even verified. We propose the concept of mandatory neurons and highlight their importance in the robustness of model predictions. Such causal links between neurons and prediction outcomes are not only identified but also verified. We believe this "identify then verify" paradigm can be extended to existing research on NAPs to certify our understanding of neural networks. We leave the exploration of this direction for our future work.

9 CONCLUSION

We introduce a new problem – learning the minimal NAP specification, and discuss its importance in neural network verification. Finding minimal NAP specification not only enables the verification of larger input regions compared to existing methods but also provides a means of inspecting when and how neural networks can make reliable and robust predictions. To solve this problem, we first propose two simple approaches `REFINE` and `COARSEN`, which leverage off-the-shelf verification tools that find the minimal NAP specification with correctness guarantees. We also propose the statistical version of `REFINE` and `COARSEN`, that combine sampling and statistical learning principles to achieve correctness in an more efficient manner. However, these approaches depend on underlying verification tools that are computationally expensive. To this end, we propose two approximate approaches, `ADVERSARIAL_PRUNE` and `GRADIENT_SEARCH`. These methods utilize adversarial attacks and local gradient computation to efficiently investigate potential causal relationships between specific neurons and the model's robustness. Finally, to appreciate the volumetric change from the most refined NAPs to the minimal NAPs, we propose a simple method for estimating the volume of the region corresponding to a NAP. Our experiments indicate that minimal NAP specifications utilize much smaller fractions of neurons compared to the most refined NAPs. Nevertheless, they enable a substantial expansion of the verifiable boundaries by several orders of magnitude.

REFERENCES

David Alvarez Melis and Tommi Jaakkola. 2018. Towards robust interpretability with self-explaining neural networks. *Advances in neural information processing systems* 31 (2018).

David Bau, Bolei Zhou, Aditya Khosla, Aude Oliva, and Antonio Torralba. 2017. Network Dissection: Quantifying Interpretability of Deep Visual Representations. In *2017 IEEE Conference on Computer Vision and Pattern Recognition, CVPR 2017, Honolulu, HI, USA, July 21–26, 2017*. IEEE Computer Society, 3319–3327. <https://doi.org/10.1109/CVPR.2017.354>

Alex Bäuerle, Daniel Jönsson, and Timo Ropinski. 2022. Neural Activation Patterns (NAPs): Visual Explainability of Learned Concepts. *CoRR* abs/2206.10611 (2022). <https://doi.org/10.48550/arXiv.2206.10611> arXiv:2206.10611

Yoshua Bengio, Aaron Courville, and Pascal Vincent. 2013. Representation Learning: A Review and New Perspectives. *IEEE Transactions on Pattern Analysis and Machine Intelligence* 35, 8 (2013), 1798–1828. <https://doi.org/10.1109/TPAMI.2013.50>

Akhilan Boopathy, Sijia Liu, Gaoyuan Zhang, Cynthia Liu, Pin-Yu Chen, Shiyu Chang, and Luca Daniel. 2020. Proper network interpretability helps adversarial robustness in classification. In *International Conference on Machine Learning*. PMLR, 1014–1023.

Christopher Brix, Stanley Bak, Changliu Liu, and Taylor T. Johnson. 2023. The Fourth International Verification of Neural Networks Competition (VNN-COMP 2023): Summary and Results. *CoRR* abs/2312.16760 (2023). <https://doi.org/10.48550/ARXIV.2312.16760> arXiv:2312.16760

N. Carlini and D. Wagner. 2017. Towards Evaluating the Robustness of Neural Networks. In *2017 IEEE Symposium on Security and Privacy (SP)*. IEEE Computer Society, Los Alamitos, CA, USA, 39–57. <https://doi.org/10.1109/SP.2017.49>

Chih-Hong Cheng, Georg Nührenberg, and Harald Ruess. 2017. Maximum Resilience of Artificial Neural Networks. In *Automated Technology for Verification and Analysis - 15th International Symposium, ATVA 2017, Pune, India, October 3-6, 2017, Proceedings (Lecture Notes in Computer Science, Vol. 10482)*, Deepak D’Souza and K. Narayan Kumar (Eds.). Springer, 251–268. https://doi.org/10.1007/978-3-319-68167-2_18

Patrick Cousot and Radhia Cousot. 1977. Abstract Interpretation: A Unified Lattice Model for Static Analysis of Programs by Construction or Approximation of Fixpoints. In *Conference Record of the Fourth ACM Symposium on Principles of Programming Languages, Los Angeles, California, USA, January 1977*, Robert M. Graham, Michael A. Harrison, and Ravi Sethi (Eds.). ACM, 238–252. <https://doi.org/10.1145/512950.512973>

Patrick Cousot and Radhia Cousot. 2014. Abstract interpretation: past, present and future. In *Joint Meeting of the Twenty-Third EACSL Annual Conference on Computer Science Logic (CSL) and the Twenty-Ninth Annual ACM/IEEE Symposium on Logic in Computer Science (LICS), CSL-LICS '14, Vienna, Austria, July 14 - 18, 2014*, Thomas A. Henzinger and Dale Miller (Eds.). ACM, 2:1–2:10. <https://doi.org/10.1145/2603088.2603165>

Thomas G. Dietterich and Eric Horvitz. 2015. Rise of concerns about AI: reflections and directions. *Commun. ACM* 58, 10 (2015), 38–40. <https://doi.org/10.1145/2770869>

Yinpeng Dong, Hang Su, Jun Zhu, and Fan Bao. 2017. Towards interpretable deep neural networks by leveraging adversarial examples. *arXiv preprint arXiv:1708.05493* (2017).

Martin E. Dyer and Alan M. Frieze. 1988. On the Complexity of Computing the Volume of a Polyhedron. *SIAM J. Comput.* 17, 5 (1988), 967–974. <https://doi.org/10.1137/0217060>

Rüdiger Ehlers. 2017. Formal Verification of Piece-Wise Linear Feed-Forward Neural Networks. *CoRR* abs/1705.01320 (2017). arXiv:1705.01320 <http://arxiv.org/abs/1705.01320>

D. Erhan, Yoshua Bengio, Aaron C. Courville, and Pascal Vincent. 2009. Visualizing Higher-Layer Features of a Deep Network.

Jonathan Frankle and Michael Carbin. 2019. The Lottery Ticket Hypothesis: Finding Sparse, Trainable Neural Networks. In *7th International Conference on Learning Representations, ICLR 2019, New Orleans, LA, USA, May 6–9, 2019*. OpenReview.net. <https://openreview.net/forum?id=rJL-b3RcF7>

Timon Gehr, Matthew Mirman, Dana Drachsler-Cohen, Petar Tsankov, Swarat Chaudhuri, and Martin Vechev. 2018. AI2: Safety and Robustness Certification of Neural Networks with Abstract Interpretation. In *2018 IEEE Symposium on Security and Privacy (SP)*. 3–18. <https://doi.org/10.1109/SP.2018.00058>

Chuqin Geng, Nham Le, Xiaojie Xu, Zhaoyue Wang, Arie Gurfinkel, and Xujie Si. 2023. Towards Reliable Neural Specifications. In *International Conference on Machine Learning, ICML 2023, 23–29 July 2023, Honolulu, Hawaii, USA (Proceedings of Machine Learning Research, Vol. 202)*, Andreas Krause, Emma Brunskill, Kyunghyun Cho, Barbara Engelhardt, Sivan Sabato, and Jonathan Scarlett (Eds.). PMLR, 11196–11212. <https://proceedings.mlr.press/v202/geng23a.html>

Chuqin Geng, Xiaojie Xu, Haolin Ye, and Xujie Si. 2022. Scalar Invariant Networks with Zero Bias. *CoRR* abs/2211.08486 (2022). <https://doi.org/10.48550/ARXIV.2211.08486> arXiv:2211.08486

Ian J. Goodfellow, Jonathon Shlens, and Christian Szegedy. 2015. Explaining and Harnessing Adversarial Examples. In *3rd International Conference on Learning Representations, ICLR 2015, San Diego, CA, USA, May 7–9, 2015, Conference Track Proceedings*, Yoshua Bengio and Yann LeCun (Eds.). <http://arxiv.org/abs/1412.6572>

Divya Gopinath, Kaiyuan Wang, Mengshi Zhang, Corina S. Pasareanu, and Sarfraz Khurshid. 2018. Symbolic Execution for Deep Neural Networks. *CoRR* abs/1807.10439 (2018). arXiv:1807.10439 <http://arxiv.org/abs/1807.10439>

Boris Hanin and David Rolnick. 2019a. Complexity of Linear Regions in Deep Networks. In *ICML (Proceedings of Machine Learning Research, Vol. 97)*. PMLR, 2596–2604.

Boris Hanin and David Rolnick. 2019b. Deep ReLU Networks Have Surprisingly Few Activation Patterns. In *NeurIPS*. 359–368.

Xiaowei Huang, Daniel Kroening, Wenjie Ruan, James Sharp, Youcheng Sun, Emese Thamo, Min Wu, and Xinping Yi. 2020. A survey of safety and trustworthiness of deep neural networks: Verification, testing, adversarial attack and defence, and interpretability. *Comput. Sci. Rev.* 37 (2020), 100270. <https://doi.org/10.1016/j.cosrev.2020.100270>

Xiaowei Huang, Marta Kwiatkowska, Sen Wang, and Min Wu. 2017a. Safety Verification of Deep Neural Networks. In *Computer Aided Verification - 29th International Conference, CAV 2017, Heidelberg, Germany, July 24–28, 2017, Proceedings, Part I (Lecture Notes in Computer Science, Vol. 10426)*, Rupak Majumdar and Viktor Kuncak (Eds.). Springer, 3–29. https://doi.org/10.1007/978-3-319-63387-9_1

Xiaowei Huang, Marta Kwiatkowska, Sen Wang, and Min Wu. 2017b. Safety Verification of Deep Neural Networks. In *Computer Aided Verification - 29th International Conference, CAV 2017, Heidelberg, Germany, July 24–28, 2017, Proceedings, Part I (Lecture Notes in Computer Science, Vol. 10426)*, Rupak Majumdar and Viktor Kuncak (Eds.). Springer, 3–29. https://doi.org/10.1007/978-3-319-63387-9_1

Guy Katz, Clark W. Barrett, David L. Dill, Kyle Julian, and Mykel J. Kochenderfer. 2017. Reluplex: An Efficient SMT Solver for Verifying Deep Neural Networks. In *Computer Aided Verification - 29th International Conference, CAV 2017, Heidelberg, Germany, July 24–28, 2017, Proceedings, Part I (Lecture Notes in Computer Science, Vol. 10426)*, Rupak Majumdar and Viktor Kuncak (Eds.). Springer, 97–117. https://doi.org/10.1007/978-3-319-63387-9_5

Guy Katz, Derek A. Huang, Dulgur Ibeling, Kyle Julian, Christopher Lazarus, Rachel Lim, Parth Shah, Shantanu Thakoor, Haoze Wu, Aleksandar Zeljic, David L. Dill, Mykel J. Kochenderfer, and Clark W. Barrett. 2019. The Marabou Framework for Verification and Analysis of Deep Neural Networks. In *Computer Aided Verification - 31st International Conference, CAV 2019, New York City, NY, USA, July 15–18, 2019, Proceedings, Part I (Lecture Notes in Computer Science, Vol. 11561)*, Isil Dillig and Serdar Tasiran (Eds.). Springer, 443–452. https://doi.org/10.1007/978-3-030-25540-4_26

Zhaoyu Li, Jinpei Guo, Yuhe Jiang, and Xujie Si. 2023. Learning Reliable Logical Rules with SATNet. In *Advances in Neural Information Processing Systems 36: Annual Conference on Neural Information Processing Systems 2023, NeurIPS 2023, New Orleans, LA, USA, December 10 - 16, 2023*, Alice Oh, Tristan Naumann, Amir Globerson, Kate Saenko, Moritz Hardt, and Sergey Levine (Eds.). http://papers.nips.cc/paper_files/paper/2023/hash/2ff46d83d1dcc063e075058b29d55efe-Abstract-Conference.html

Percy Liang, Omer Tripp, and Mayur Naik. 2011. Learning minimal abstractions. In *Proceedings of the 38th ACM SIGPLAN-SIGACT Symposium on Principles of Programming Languages, POPL 2011, Austin, TX, USA, January 26–28, 2011*, Thomas Ball and Mooly Sagiv (Eds.). ACM, 31–42. <https://doi.org/10.1145/1926385.1926391>

Tailin Liang, John Glossner, Lei Wang, Shaobo Shi, and Xiaotong Zhang. 2021. Pruning and quantization for deep neural network acceleration: A survey. *Neurocomputing* 461 (2021), 370–403. <https://doi.org/10.1016/J.NEUCOM.2021.07.045>

Jingyue Lu and M. Pawan Kumar. 2019. Neural Network Branching for Neural Network Verification. *CoRR* abs/1912.01329 (2019). arXiv:1912.01329 <http://arxiv.org/abs/1912.01329>

Lu Lu, Yeonjong Shin, Yanhui Su, and George E. Karniadakis. 2019. Dying ReLU and Initialization: Theory and Numerical Examples. *CoRR* abs/1903.06733 (2019). arXiv:1903.06733 <http://arxiv.org/abs/1903.06733>

Anna Lukina, Christian Schilling, and Thomas A. Henzinger. 2021. Into the Unknown: Active Monitoring of Neural Networks. In *Runtime Verification - 21st International Conference, RV 2021, Virtual Event, October 11–14, 2021, Proceedings (Lecture Notes in Computer Science, Vol. 12974)*, Lu Feng and Dana Fisman (Eds.). Springer, 42–61. https://doi.org/10.1007/978-3-03-88494-9_3

Aleksander Madry, Aleksandar Makelov, Ludwig Schmidt, Dimitris Tsipras, and Adrian Vladu. 2018. Towards Deep Learning Models Resistant to Adversarial Attacks. In *6th International Conference on Learning Representations, ICLR 2018, Vancouver, BC, Canada, April 30 - May 3, 2018, Conference Track Proceedings*. OpenReview.net. <https://openreview.net/forum?id=rJzIBZAb>

Matthew Mirman, Timon Gehr, and Martin T. Vechev. 2018. Differentiable Abstract Interpretation for Provably Robust Neural Networks. In *International Conference on Machine Learning*. <https://api.semanticscholar.org/CorpusID:51872670>

Ramprasaath R. Selvaraju, Abhishek Das, Ramakrishna Vedantam, Michael Cogswell, Devi Parikh, and Dhruv Batra. 2017. Grad-CAM: Visual Explanations from Deep Networks via Gradient-Based Localization. In *2017 IEEE International Conference on Computer Vision (ICCV)*. 618–626. <https://doi.org/10.1109/ICCV.2017.74>

Yuval Shapira, Eran Avneri, and Dana Drachsler-Cohen. 2023. Deep Learning Robustness Verification for Few-Pixel Attacks. *Proc. ACM Program. Lang.* 7, OOPSLA1, Article 90 (apr 2023), 28 pages. <https://doi.org/10.1145/3586042>

Karen Simonyan, Andrea Vedaldi, and Andrew Zisserman. 2014. Deep Inside Convolutional Networks: Visualising Image Classification Models and Saliency Maps. In *2nd International Conference on Learning Representations, ICLR 2014, Banff, AB, Canada, April 14–16, 2014, Workshop Track Proceedings*, Yoshua Bengio and Yann LeCun (Eds.). <http://arxiv.org/abs/1312.6034>

Karen Simonyan and Andrew Zisserman. 2014. Very Deep Convolutional Networks for Large-Scale Image Recognition. *CoRR* abs/1409.1556 (2014). <https://api.semanticscholar.org/CorpusID:14124313>

Naftali Tishby and Noga Zaslavsky. 2015. Deep learning and the information bottleneck principle. In *2015 ieee information theory workshop (itw)*. IEEE, 1–5.

Vincent Tjeng, Kai Yuanqing Xiao, and Russ Tedrake. 2019. Evaluating Robustness of Neural Networks with Mixed Integer Programming. In *7th International Conference on Learning Representations, ICLR 2019, New Orleans, LA, USA, May 6–9, 2019*. OpenReview.net. <https://openreview.net/forum?id=HyGIdiRqtm>

VNNCOMP. 2021. VNNCOMP. <https://sites.google.com/view/vnn2021>

Shiqi Wang, Huan Zhang, Kaidi Xu, Xue Lin, Suman Jana, Cho-Jui Hsieh, and J. Zico Kolter. 2021b. Beta-CROWN: Efficient Bound Propagation with Per-neuron Split Constraints for Neural Network Robustness Verification. In *Advances in Neural Information Processing Systems 34: Annual Conference on Neural Information Processing Systems 2021, NeurIPS 2021, December 6–14, 2021, virtual*, Marc'Aurelio Ranzato, Alina Beygelzimer, Yann N. Dauphin, Percy Liang, and Jennifer Wortman Vaughan (Eds.). 29909–29921. <https://proceedings.neurips.cc/paper/2021/hash/fac7fead96dafceaf80c1daffae82a4-Abstract.html>

Shiqi Wang, Huan Zhang, Kaidi Xu, Xue Lin, Suman Jana, Cho-Jui Hsieh, and J. Zico Kolter. 2021c. Beta-CROWN: Efficient Bound Propagation with Per-neuron Split Constraints for Neural Network Robustness Verification. In *Advances in Neural Information Processing Systems 34: Annual Conference on Neural Information Processing Systems 2021, NeurIPS 2021, December 6–14, 2021, virtual*, Marc'Aurelio Ranzato, Alina Beygelzimer, Yann N. Dauphin, Percy Liang, and Jennifer Wortman Vaughan (Eds.). 29909–29921. <https://proceedings.neurips.cc/paper/2021/hash/fac7fead96dafceaf80c1daffae82a4-Abstract.html>

Zi Wang, Chengcheng Li, and Xiangyang Wang. 2021a. Convolutional Neural Network Pruning With Structural Redundancy Reduction. In *IEEE Conference on Computer Vision and Pattern Recognition, CVPR 2021, virtual, June 19–25, 2021*. Computer Vision Foundation / IEEE, 14913–14922. <https://doi.org/10.1109/CVPR46437.2021.01467>

Jeannette M. Wing. 1990. A Specifier’s Introduction to Formal Methods. *Computer* 23, 9 (1990), 8–24. <https://doi.org/10.1109/2.58215>

William Wolberg, Olvi Mangasarian, Nick Street, and W. Street. 1995. Breast Cancer Wisconsin (Diagnostic). UCI Machine Learning Repository. DOI: <https://doi.org/10.24432/C5DW2B>.

Han Xu, Yao Ma, Haochen Liu, Debayan Deb, Hui Liu, Jiliang Tang, and Anil K. Jain. 2020. Adversarial Attacks and Defenses in Images, Graphs and Text: A Review. *Int. J. Autom. Comput.* 17, 2 (2020), 151–178. <https://doi.org/10.1007/s11633-019-1211-x>

Kaidi Xu, Huan Zhang, Shiqi Wang, Yihan Wang, Suman Jana, Xue Lin, and Cho-Jui Hsieh. 2021. Fast and Complete: Enabling Complete Neural Network Verification with Rapid and Massively Parallel Incomplete Verifiers. In *9th International Conference on Learning Representations, ICLR 2021, Virtual Event, Austria, May 3–7, 2021*. OpenReview.net. <https://openreview.net/forum?id=nVZtXB16LNn>

Jason Yosinski, Jeff Clune, Anh Mai Nguyen, Thomas J. Fuchs, and Hod Lipson. 2015. Understanding Neural Networks Through Deep Visualization. *CoRR* abs/1506.06579 (2015). arXiv:1506.06579 <http://arxiv.org/abs/1506.06579>

Yu Zhang, Peter Tiño, Ales Leonardis, and Ke Tang. 2021. A Survey on Neural Network Interpretability. *IEEE Trans. Emerg. Top. Comput. Intell.* 5, 5 (2021), 726–742. <https://doi.org/10.1109/TETCI.2021.3100641>

A PROOFS OF SIMPLE APPROACHES

Theorem A.1 (Property of *REFINE*). *The algorithm *REFINE* returns a minimal NAP specification with $O(2^{|N|})$ calls to \mathcal{V} .*

PROOF. Let P be the returned NAP. We prove this by contradiction. Suppose we can further refine P , meaning there exists a NAP P' such that $|P'| \leq |P|$ and $\mathcal{V}(P') = 1$. However, the algorithm states that any P' smaller than $|P|$ fails verification, which contradicts $\mathcal{V}(P') = 1$.

In the worst case, the NAP size k runs up to $|N|$. For each k , we need to check $\binom{|N|}{k}$ number of NAPs. In total, this number of NAPs we need to check is $\binom{|N|}{1} + \binom{|N|}{2} + \dots + \binom{|N|}{|N|} = 2^{|N|} - 1$ according to the binomial theorem, resulting in a runtime complexity of $O(2^{|N|})$. \square

Theorem A.2 (Property of *COARSEN*). *The algorithm *COARSEN* returns a minimal NAP specification with $O(|N|)$ calls to \mathcal{V} .*

PROOF. Let P be the NAP returned by *COARSEN*. Our goal is to show that any P' smaller than P results in $\mathcal{V}(P') = 0$. To construct such a smaller P' , we need to apply the refine action $\tilde{\Delta}$ on P through some neuron $N_{i,l}$, i.e., $P' := \tilde{\Delta}(N_{i,l}) = \tilde{\mathcal{A}}(N_{i,l}) \cup P \setminus P_{i,l}$. According to the algorithm, $\mathcal{V}(P') = 0$. In the worst case, the algorithm needs to iterate through each neuron in N , resulting in a runtime complexity of $O(|N|)$. \square

B PROOFS OF STATISTICAL APPROACHES

Our proofs of properties of *SAMPLE_REFINE* and *SAMPLE_COARSEN* mainly follow those in [Liang et al. 2011]. Interested readers may refer to it for detailed proofs.

Theorem B.1 (Property of *SAMPLE_REFINE*). *With probability $\theta = |(\frac{|M|}{|M|+1})|^{|M|}$, *SAMPLE_REFINE* has $1 - \delta$ probability of outputting a minimal NAP specification with $\Theta(|M|^2(\log |N| + \log(s/\delta)))$ examples each iteration and $O(s|M|^2(\log |N| + \log(s/\delta)))$ total calls to \mathcal{V} .*

PROOF. Considering the size of the minimal specification s , *SAMPLE_REFINE* will execute s iterations. If we sample k times in each iteration, then the probability of selecting a mandatory neuron is at least $1 - \frac{\delta}{s}$. Consequently, by applying a union bound, the algorithm will identify a NAP specification with a probability of at least $1 - \delta$.

Now, let's delve deeper into one iteration of the process. The fundamental concept is that a mandatory neuron m demonstrates a stronger correlation with proving the robustness query ($\mathcal{V}(P) = 1$) compared to a non-mandatory one. This enhanced correlation increases the probability of its selection significantly when k is sufficiently large.

Let's revisit the notion of M , representing the set of mandatory neurons with a size of $|M|$. Now, let's focus on a specific mandatory neuron $n^+ \in M$. We define B_{j-} as the event indicating $k_{n^-} > k_{n^+}$, and B as the event where B_{j-} holds for any non-mandatory neuron $n^- \in N \setminus M$. Importantly, if B fails to occur, then the algorithm will correctly identify a mandatory neuron. Hence, our primary objective is to establish that $Pr(B) \leq \frac{\delta}{s}$. Initially, employing a union bound provides:

$$Pr(B) \leq \sum_{n^-} Pr(B_{n^-}) \leq |N| \max_{n^-} Pr(B_{n^-}) \quad (15)$$

Let's delve into each training example $P^{(i)}$ and introduce the notation $X_i = (1 - \mathcal{V}(P^{(i)}))(P_{n^-}^{(i)} - P_{n^+}^{(i)})$. It's worth emphasizing that B_{n^-} manifests precisely when $\frac{1}{n}(k_{n^-} - k_{n^+}) = \frac{1}{n} \sum_{i=1}^n X_i > 0$. Our objective now is to bound this quantity utilizing Hoeffding's inequality, considering the mean as:

$$\mathbb{E}[X_i] = Pr(\mathcal{V}(P) = 1, P_{n^-} \in \{1, 0\}) - Pr(\mathcal{V}(P) = 1, P_{n^+} \in \{1, 0\}) \quad (16)$$

and the bounds are $-1 \leq \mathbb{E}[X_i] \leq 1$. Setting $\epsilon = -\mathbb{E}[X_i]$, we get:

$$\Pr(B_{n^-}) \leq e^{-\frac{k\epsilon^2}{2}}, n^+ \in M, n^- \notin M. \quad (17)$$

Substituting (16) into (15) and rearranging terms, we can solve for k :

$$\frac{\delta}{s} \leq |N|e^{-\frac{k\epsilon^2}{2}} \text{ implies } k \geq \frac{2(\log|N| + \log(\frac{s}{\delta}))}{\epsilon^2} \quad (18)$$

Our attention now shifts towards deriving a lower bound for ϵ , which intuitively reflects the discrepancy (in terms of correlation with proving the robustness query) between a mandatory neuron and a non-mandatory one. It's noteworthy that $\Pr(P_n \in \{1, 0\}) = \theta$ for any $n \in N$. Furthermore, since n^- is non-mandatory, we can assert that $\Pr(\mathcal{V}(P) = 1 | P_{n^-} \in \{1, 0\}) = \Pr(\mathcal{V}(P) = 1)$. By leveraging these observations, we can express:

$$\epsilon = \theta(\Pr(\mathcal{V}(P) = 1 | P_{n^+} \in \{1, 0\}) - \Pr(\mathcal{V}(P) = 1)) \quad (19)$$

Let's view C as the collection of minimal NAP specifications. We can treat C as a set of clauses in a Disjunctive Normal Form (DNF) formula: $\mathcal{V}(P; C) = \neg \bigvee_{c \in C} \bigwedge_{n \in c} P_n$, where we explicitly specify the dependence of \mathcal{V} on the clauses C . For example, if $C = 1, 2, 3$, it corresponds to $\mathcal{V}(P) = \neg[(P_1 \wedge P_2) \vee P_3]$. Now, let $C_j = c \in C : n \in c$ denote the clauses containing n . We reformulate $\Pr(\mathcal{V}(P) = 1)$ as the sum of two components: one originating from the mandatory neuron n^+ and the other from the non-mandatory neuron:

$$\Pr(\mathcal{V}(P) = 1) = \Pr(\mathcal{V}(P; C_{n^+}) = 1, \mathcal{V}(P; C \setminus C_{n^+}) = 0) \quad (20)$$

$$+ \Pr(\mathcal{V}(P; C \setminus C_{n^+}) = 1) \quad (21)$$

Calculating $\Pr(\mathcal{V}(P) = 1 | P_{n^+} \in \{1, 0\})$ follows a similar process. The only distinction arises from conditioning on $P_{n^+} \in \{1, 0\}$, which introduces an extra factor of $\frac{1}{\theta}$ in the first term because conditioning divides by $\Pr(P_{n^+}) = \theta$. The second term remains unchanged since no $c \notin C_{n^+}$ is mandatory in P_{n^+} . Substituting these two outcomes back into the equation yields:

$$\epsilon = (1 - \theta)\Pr(\mathcal{V}(P; C_{n^+}) = 1, \mathcal{V}(P; C \setminus C_{n^+}) = 0) \quad (22)$$

Now, our objective is to establish a lower bound for (22) across all possible \mathcal{V} (equivalently, C), where n^+ is permitted to be mandatory in C . Interestingly, the worst possible C can be obtained by either having $|M|$ disjoint clauses ($C = n : n \in M$) or a single clause ($C = M$ if $s = |M|$). The intuition behind this is that when C consists of $|M|$ clauses, there are numerous possibilities ($|M| - 1$ of them) for some $c \notin C_{n^+}$ to be true, making it challenging to determine that n^+ is a mandatory neuron; in such cases, $\epsilon = (1 - \theta)\theta(1 - \theta)^{|M|-1}$. Conversely, if C comprises a single clause, then letting this clause be true becomes exceedingly challenging; in this scenario, $\epsilon = (1 - \theta)\theta^{|M|}$.

Let's consider the scenario where C comprises $|M|$ clauses. We aim to maximize ϵ concerning θ by setting the derivative $\frac{d\epsilon}{d\theta} = 0$ and solving for θ . This optimization yields $\theta = \frac{1}{|M|+1}$ as the optimal value. Substituting this value into the formula of ϵ , we obtain $\epsilon = \frac{1}{|M|+1} \left(\frac{|M|}{|M|+1} \right)^{|M|}$. Note that $\left(\frac{|M|}{|M|+1} \right)^{|M|}$ can be lower bounded by e^{-1} , implying that $\epsilon^{-2} = O(|M|^2)$. Substituting this result to equation (18) will conclude the proof. \square

Theorem B.2 (Property of SAMPLE_COARSEN). *With probability $\theta = e^{-\frac{1}{s}}$, SAMPLE_COARSEN learns a minimal NAP specification with $O(s \log|N|)$ calls to \mathcal{V} .*

PROOF. Let's first estimate the number of calls that SAMPLE_COARSEN makes to \mathcal{V} . We denote the number of calls as $C(P^L)$, where P^L is the most refined NAP. Then $C(P^L)$ can be computed

recursively using the following rule:

$$C(P^L) = \begin{cases} |P| & \text{if } |P^L| \leq s+1 \\ 1 + \mathbb{E}[(1 - \mathcal{V}(P))C(P) + \mathcal{V}(P)C(P^L)] & \text{otherwise} \end{cases} \quad (23)$$

where P is the sampled NAP. By assumption, there exists a NAP $P^S \preccurlyeq P$ of size s that passes the verification. Define $G(P) = \neg(P^S \preccurlyeq P)$, which is 0 when P^S subsumes P , i.e., all mandatory neurons in P^S shows up in the sampled P . This follows that $\Pr(G(P) = 0) = \Pr(P^S \preccurlyeq P) = \theta^s$. Note that $G(P) \geq \mathcal{V}(P)$, as the NAP P^S suffices to prove the robustness query. We can estimate the upper bound of $C(P^L)$ by replacing \mathcal{V} with G :

$$C(P^L) \leq 1 + \mathbb{E}[(1 - G(P))C(P) + G(P)C(P^L)] \quad (24)$$

$$\leq 1 + \theta^s \mathbb{E}[C(P)|P^S \preccurlyeq P] + (1 - \theta^s)C(P^L) \quad (25)$$

$$\leq \mathbb{E}[C(P)|P^S \preccurlyeq P] + \theta^{-s} \quad (26)$$

We now denote $C(n) = \max_{|P|=n} C(P)$ as the maximum over NAP of size n . Note that given $P^S \preccurlyeq P$, $|P| = s + N$ where N is a binomial random variable with $\mathbb{E}(N) = \theta(n - s)$.

Using the bound $C(n) \leq (1 - \theta^n)C(n-1) + \theta^n C(n)\theta^{-s}$, we can observe that $C(n) \leq \frac{\theta^{-s}}{1-\theta^n} \cdot n$. In addition, when n is large enough, $C(n)$ is concave, then by use Jensen's inequality:

$$C(n) \leq C(\mathbb{E}[s + N]) + \theta^{-s} = C(s + \theta(n - s)) + \theta^{-s} \quad (27)$$

To solve the recurrence, this gives us:

$$C(n) \leq \frac{\theta^{-s} \log n}{\log \theta^{-1}} + s + 1 \quad (28)$$

The equation above illustrates a tradeoff between reducing the number of iterations (by increasing $\log \theta^{-1}$) and reducing the number of samples (by decreasing θ^{-s}). To minimize $C(n)$, we need to set θ so that the gradient of $C(n)$ w.r.t θ^{-1} is 0. This gives us: $\frac{s x^{s-1}}{\log x} - \frac{x^{s-1}}{\log^2 x} = 0$, solving this gives us $\theta = e^{-\frac{1}{s}}$. Consequently, the upper bound becomes $C(n) = es \log n + s + 1 = O(s \log n)$. \square

Received 20 February 2007; revised 12 March 2009; accepted 5 June 2009